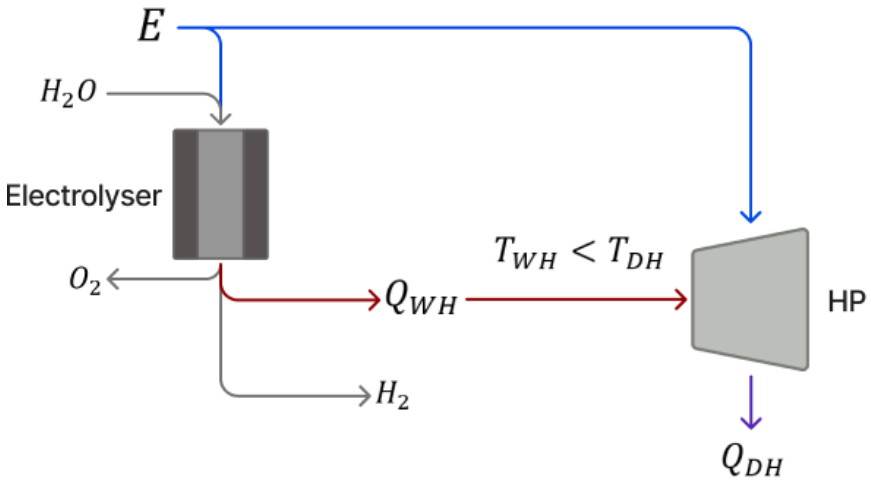

Techno-economic assessment of Waste Heat Recovery from electrolyser plants and its application in District Heating networks

A Gothenburg case study

Master's thesis in Master Programme Sustainable Energy Systems

Cajsa Jacobsson
Hugo Palmgren

DEPARTMENT OF SPACE, EARTH AND ENVIRONMENT
CHALMERS UNIVERSITY OF TECHNOLOGY
Gothenburg, Sweden 2025
www.chalmers.se

Master's thesis 2025

Techno-economic assessment of waste heat recovery from electrolyser plants and its application in district heating networks

Cajsa Jacobsson
Hugo Palmgren

CHALMERS
UNIVERSITY OF TECHNOLOGY

Department of Space, Earth and Environment
Division of Energy Technology
Chalmers University of Technology
Gothenburg, Sweden 2025

Assessing Cost-Effectiveness of Waste Heat Utilization from Hydrogen Production in Electrolysers in Future Gothenburg District Heating System

Master´s Thesis in the Master Program Sustainable Energy Systems

Cajsa Jacobsson
Hugo Palmgren

Supervisor: Oscar Hult, Sigholm Tech
Supervisor: Per Ringqvist, Sigholm Tech
Supervisor: Alla Toktarova, Chalmers University of Technology
Supervisor: Hyunkyo Yu, Chalmers University of Technology
Examiner: Lisa Göransson, Chalmers University of Technology

Master's Thesis 2025
Department of Space, Earth and Environment
Division of Energy Technology
Chalmers University of Technology
SE-412 96 Gothenburg
Telephone +46 31 772 1000

Cover: Schematic visualization of the mass and heat flows of a waste heat recovery system connected to an electrolyser.

Typeset in LaTeX
Printed by Chalmers Reproservice
Gothenburg, Sweden 2025

Abstract

With the EU aiming for carbon neutrality by 2050, electricity-based hydrogen production via electrolysis is gaining importance. As this process generates excess heat, waste heat recovery (WHR) from electrolysers presents an opportunity to improve energy efficiency and lower heating and hydrogen costs. This study investigates the integration of electrolyser waste heat into Gothenburg's district heating system and explores the cost-optimal energy system configuration for 2050. A linear programming model was used to minimise the total system cost, considering two types of electrolysers: Alkaline (AEL) and Proton Exchange Membrane (PEM), as well as waste heat recovery technologies such as heat exchangers (HX) and heat pumps (HP). The analysis included scenarios with and without WHR, varied electrolyser options, and sensitivity analyses.

Results show that WHR reduces system, heat, and hydrogen costs. The model favoured investments in HX for AEL at 90°C and HPs for AEL/PEM at 80°C, replacing conventional heat sources. Electrolyser type influenced investment and operation patterns, though differences in total cost were small. Sensitivity analysis revealed that taxes on power-to-heat (PtH) technologies affect heat production choices. A tax applied to all PtH technologies increases system costs and the share of thermal generation, whereas a tax on individual heat pumps yields similar costs compared to a case without a PtH tax, but eliminates all generation from individual heat pumps. TES reduces costs, and hydrogen storage improves electrolyser flexibility and reduces the need for peaking heat units.

In conclusion, the results of this thesis show that WHR integration is technically and economically beneficial to the Gothenburg energy system in 2050. It also highlights the importance of technology choices and coordination between hydrogen and district heating actors.

Keywords: Waste Heat Recovery (WHR), Electrolysers, District Heating, Hydrogen Production, Alkaline Electrolyser (AEL), Proton Exchange Membrane (PEM), Linear Programming, Heat Pumps (HP), Heat Exchangers (HX).

Acknowledgements

This thesis could not have happened if it weren't for the incredible support we've received along the way. First and foremost, we want to thank all four of our supervisors for being the best we could have ever hoped for. So, in alphabetical order; Alla, thank you for your dedication and for all of the laughs we shared along the way, you really pushed us further than we ever could have gotten on our own. Hyunkyo, thank you for allowing us to work with your model and for your non-stop support when we had (so many) questions, we definitely don't take it for granted. Thank you Oscar for your honesty and critical eye, without your insights, this project would have undoubtedly lacked a perspective that we truly believe elevates its content. And finally Per, thank you for all the fruitful discussions you raised throughout this project, you undoubtedly made not only the content, but us better for it. We would also like to dedicate a big thank you to Lisa for the trust you've shown us, not only in terms of this thesis, but also as your teaching assistants.

Furthermore, we want to dedicate a big thank you to all of the people at Sigholm for not only being welcoming, but also for the genuine interest you showed in us and our work. You would be hard pressed to find a more welcoming environment and we are thankful that we got to spend our time writing this report with you. Lastly, we want to thank all the people at the department of SEE, not least the people that in ways contributed to this work, for your time, interest and most importantly; the fika.

Cajsa Jacobsson and Hugo Palmgren, Gothenburg, May 2025

List of Acronyms

Below is the list of acronyms that have been used throughout this thesis listed in alphabetical order:

AEL	Alkaline electrolyser
AELX	Alkaline electrolyser operating at X°C
AEM	Anion exchange membrane electrolyser technologies
BoP	Balance of Plant
CCS	Carbon Capture and Storage
CCU	Carbon Capture and Utilisation
CHP	Combined Heat and Power
DH	District Heating
EB	Electric Boiler
EC	European Commission
EU	European Union
GHG	Greenhouse Gas
HHV	Higher Heating Value
HOB	Heat Only Boiler
HP	Heat Pump
HX	Heat Exchanger
LHV	Lower Heating Value
LP	Linear Programming
MSW	Municipal Solid Waste
O&M	Operation and Maintenance
PEM	Proton Exchange Membrane
PEMX	Proton Exchange Membrane electrolyser operating at X°C
PTH	Power to Heat
SMR	Steam Methane Reforming
SOEC	Solid Oxide Electrolysis Cell
TES	Thermal Energy Storage
WHR	Waste Heat Recovery
WtE	Waste-to-Energy

Nomenclature

Below is the nomenclature of indices, sets, parameters, and variables that have been used throughout this thesis.

Sets and Indices

Notation	Description
E	Set of electricity regions
H	Set of heating regions
I	Set of all technologies
I_{el}	Set of electricity generation technologies
I_{elec}	Set of electrolyser technologies
$I_{elec,\ AEL}$	Subset of AEL-type electrolysers
I_{HaP}	Set of heating technologies producing electricity
I_{heat}	Set of heat generation technologies
$I_{HP,WHR}$	Set of WHR heat pump units
$I_{HX,WHR}$	Set of WHR heat exchanger units
I_{pth}	Set of heating technologies with electricity input
I_{TES}	Set of TES units
T	Set of time periods

Parameters and Constants

Notation	Description
a	Cost scaling exponent for heat exchanger sizing
A_{table}	Reference surface area of heat exchanger
C_{HX}	Cost of heat exchanger per unit of transferred heat capacity
$C_{HX\ table}$	Reference cost of a standard heat exchanger
$C_{HX,\ tot}$	Total installed cost of the heat exchanger
C_i^{inv}	Investment cost of technology i
$C_i^{OM_{fix}}$	Fixed O&M cost of technology i
C_i^{run}	Running (variable) cost of technology i
C_i^{tax}	tax on generation, technology i

Notation	Description
C_t^{imp}	Cost of imported electricity at time t
$c_{i,t}^{part_{load}}$	Part-load cost of technology i at time t
$c_{i,t}^{start}$	Start-up cost of technology i at time t
$\mathrm{C}_{\mathrm{USD,\ EUR}}^{\mathrm{rate}}$	Currency conversion rate (USD to EUR)
COP_{carnot}	Theoretical maximum COP of a heat pump
$D_{e,t}^{el}$	Electricity demand in region e at time t
$D_{h,t}^{H_2}$	H_2 demand in region h at time t
$D_{h,t}^{heat}$	Heat demand in region h at time t
E_e	Electrical energy output from the WtE plant
E_h	Thermal energy output from the WtE plant
E_p	Energy attributed to the combustion of the plastic content in waste
E_{ref}	Reference electrical energy input of the electrolyser
f_p	Fraction of total carbon emissions attributed to plastic in waste
γ	Temperature sensitivity factor of electrolyser energy demand
HHV_{H2}	Higher Heating Value of hydrogen
$LHV_{C,p}$	Lower Heating Value for plastic per carbon content
LHV_{H2}	Lower Heating Value of hydrogen
LHV_{w1}	Lower Heating Value for waste containing plastic
LHV_{w2}	Lower Heating Value for waste without plastic
$M_e^{El,\ cap}$	Electricity import capacity of region e
m_C	Mass of carbon in waste
m_{CO_2}	Total annual mass of CO_2 emitted by the WtE plant
m_w	Total annual mass of waste incinerated in the WtE plant
$P_{HP,\ WHR}$	Availability factor for WHR HP operation
$P_{HX,\ WHR}$	Availability factor for WHR HX operation
Q	Annual recoverable heat transferred through the heat exchanger
Q_{IC}	Heat losses in internal cooling of electrolyser
Q_{WH}	Waste heat available from electrolyser
T_{cold}	Temperature of the cold reservoir (K)
T_{hot}	Temperature of the hot reservoir (K)
T_{WH}	Actual waste heat temperature from the electrolyser (°C)
$T_{WH,ref}$	Reference waste heat temperature (°C)
T_1, T_2	Inlet and outlet temperatures on the hot side of the HX
t_1, t_2	Inlet and outlet temperatures on the cold side of the HX
U	Overall heat transfer coefficient for water-to-water heat exchange
ΔT_{lm}	Logarithmic mean temperature difference
$\Delta E_{HHV\ to\ LHV}$	Difference in energy requirement based on higher and lower heating value
η_i	Efficiency of technology i
η_i^{WHR}	Efficiency of WHR system of technology i
η_{HHV}	Efficiency based on Higher Heating Value (HHV)
η_{IC}	Efficiency of internal cooling heat transfer
η_{LHV}	Efficiency based on Lower Heating Value (LHV)
η_{WH}	fraction of electrical input converted into recoverable heat

Variables

Notation	Description
$b_{e,t}^{ch}$	Battery charging in region e at time t
$b_{e,t}^{dch}$	Battery discharging in region e at time t
C^{tot}	Total system cost to be minimized
$H2_{h,t}^{el}$	Electricity consumption for H_2 production in region h at time t
$H2_{i,h,t}^{gen}$	H_2 generation by electrolyser i in region h at time t
$\mathrm{MC}_{h,t}^{\text{heat balance}}$	Time- and region-specific marginal cost of heat balance
$\mathrm{MC}_{\mathrm{H_2}}^{\mathrm{avg}}$	Average marginal cost of hydrogen production
$\mathrm{MC}_{\mathrm{heat}}^{\mathrm{avg}}$	Average marginal cost of heat generation
$\mathrm{MC}_{t}^{H_2\ balance}$	Time-dependent marginal cost of hydrogen balance
$p_{i,e,t}$	Electricity generation from technology i in region e at time t
$q_{i,h,t}$	Heat generation from technology i in region h at time t
$s_{bat,e}$	Battery capacity in region e
$s_{bat,\ cap}$	Maximum battery charge/discharge power
$s_{h_2,h}$	H_2 storage capacity in region h
$s_{i,e}$	Installed capacity of technology i in electricity region e
$s_{i,h}$	Installed capacity of technology i in heating region h
$s_{TES,\ cap}$	Maximum TES charge/discharge power
$s_{TES,h}$	TES capacity in region h
$SOC_{e,t}^{bat}$	Battery state-of-charge in region e at time t
$SOC_{h,t}^{H_2}$	H_2 storage level in region h at time t
$SOC_{h,t}^{TES}$	TES state-of-charge in region h at time t
$TES_{i,h,t}^{ch}$	Charging of TES unit i in region h at time t
$TES_{i,h,t}^{dch}$	Discharging of TES unit i in region h at time t
$w_{e,t}^{imp}$	Imported electricity in region e at time t

Contents

List of Figures

List of Tables

1

Introduction

In 2019, the European Commission (EC) presented the European Green Deal [1, 2], which aims to make the European Union (EU) carbon neutral by 2050. Hydrogen produced through the process of electrolysis, using renewable or nuclear electricity to split water into hydrogen and oxygen, is a strategic technology for reaching carbon neutrality by 2050. Electricity-based hydrogen can replace fossil-based hydrogen for transport and industrial processes, reducing greenhouse gas emissions and environmental impact. Additionally, it can be used to produce new industrial products, such as green fertilisers and steel. Hydrogen produced through electrolysis and with the electricity stemming from renewables such as wind and solar power, is considered a flexible energy carrier, i.e., the production and storage of hydrogen allow for managing variations of electricity generation [3, 4].

The REPowerEU Strategy of 2022 [5] set out the aim of producing 10 million tonnes (i.e., 40 GW of renewable hydrogen electrolysers) in the EU and importing 10 million tonnes of renewable hydrogen to the EU by 2030. By 2050, renewable hydrogen is expected to cover around 10% of the EU's energy needs, significantly decarbonising energy-intensive industrial processes and the transport sector.

The hydrogen production process through electrolysis also generates excess heat as a byproduct. This thermal energy, which is currently wasted, represents an opportunity for energy recovery and utilisation as electrolyser capacities rise. Figure 1.1 illustrates the potential to utilise thermal energy losses, based on projected recoverable heat-loss values for proton-exchange membrane electrolysers (PEM) and alkaline electrolysers (AEL) in 2050 [6]. It is assumed that 3% of the thermal energy remains unrecoverable, denoted as Q_{IC} and the rest can be used as a source of waste heat, Q_{WH}. More details are covered in Figures 2.1a and 2.1b.

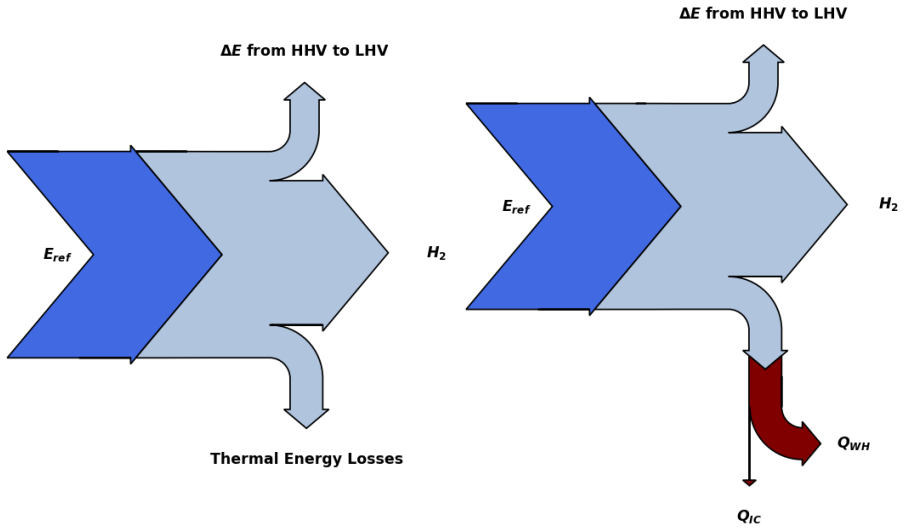

Figure 1.1: Sankey diagram displaying electrolyser energy use comparison. The right side includes WHR, while the left side does not. Thermal energy losses account for 15.9-19.9%.

Waste heat generated by electrolysers has the potential to supply heat to a diverse number of applications, such as low-temperature industry processes and building heating via district heating networks. District heating (DH) is prevalent in northern European countries like Sweden, where 50% of all homes and buildings are connected to DH networks [7]. Recovering waste heat from electrolysers and integrating it with DHs can boost the decarbonization process in the heating sector, and concurrently decrease dependency on biomass in this sector.

The potential synergies of electrolysis technologies and associated waste heat potentials and demand are elaborated in a Swedish context under consideration of national energy and climate plans. The study aims to represent the urban environment with an existing district heating network and a seasonal heat demand, such as Northern and Eastern Europe.

1.1 Aim and Scope

The aim of this project is to investigate the potential and implications of integrating waste heat from electrolysers into an existing DH network for Gothenburg.

1.1.1 Research Questions

The aim can be achieved by answering the following research questions

- How does waste heat recovery impact the cost-optimal composition of the energy system in Gothenburg?
- How does the choice of electrolyser influence the operation of heat and hydrogen generation, and what are the implications regarding the cost of heat and hydrogen?

1.2 Limitations

The model used to optimise the total system cost of the energy system of Gothenburg is a linear programming optimisation model developed in the software GAMS Studio. To maintain the linear relationships required by the model, several simplifications were necessary. One such simplification is that electricity prices are predetermined and introduced into the model through fixed profile curves. While this allows the model to maintain linearity, it also means these parameters cannot dynamically respond to changes occurring within the modelled system. For instance, a substantial rise in industrial electricity demand could, in reality, drive up the import price of electricity. Although this effect is not captured in the model, any demand exceeding the import capacity will require additional investments in domestic electricity generation.

A particularly significant simplification for the WHR analysis is the fixed Coefficient of Performance (COP) for heat pumps. In reality, the COP is non-linear and depends on the temperature difference between the heat source and the heat sink, as well as the heat pump's efficiency. Since both the heat pump's output and the DH system temperature are variables in the model, their actual relationship with COP is non-linear. To maintain linearity, the COP is fixed and parameterised in a profile curve. Heat exchangers can only operate if the waste heat is warmer than the district heating supply temperature by more than the temperature drop across the heat exchanger. This availability varies hourly based on temperatures, which is also simplified in the linear model using a profile curve.

The operation of the electrolysers is limited to their allowable load range, specifically assuming operation at or above minimum load. For Alkaline Electrolysers (AEL), this means that full shutdowns of the electrolysers are not captured by the model. This could potentially underestimate the true flexibility of electrolysers if full shutdowns are feasible in practice. The exclusion of start-up costs is a direct consequence of not fully modelling shutdown and restart behaviour. Additionally, the model's assumption of perfect foresight regarding future electricity prices and

demands allows for operational patterns that may be more extreme than those in reality. Real-world operators, facing price uncertainty, would likely use more conservative dispatch strategies, potentially leading to an overestimation of the system's flexibility and the cost savings from the resulting operation. Factors such as degradation costs and thermal inertia for electrolysers and WHR operation are also excluded, which could mask long-term performance limitations.

While assumptions about the future context of Gothenburg's energy system in 2050 are necessary, the inherent uncertainty in these long-term projections also represents a limitation on the certainty of the model's results.

1.3 Outline

The report is organised as follows. Chapter 2 covers the literature review conducted. Chapter 3 outlines the background of this work. Chapter 4 presents the methodology applied in this project. The results are presented in Chapter 5, and they are further discussed in Chapter 6. Finally, Chapter 7 summarises the conclusions drawn from the outcomes of this work.

2

Literature review

This section analyses the status and development of electrolysis technologies and their characteristics, as well as reviews the literature on waste heat recovery from the hydrogen production process.

2.1 Overview of Electrolysis Technologies

To satisfy future demands for hydrogen, electrolysis powered by renewable energy sources is considered a key technology for hydrogen production. At present, there are four main types of electrolysis technologies: alkaline (AEL), proton exchange membrane (PEM), solid oxide electrolysis cell (SOEC) and anion exchange membrane (AEM) electrolyser technologies. These technologies differ based on various physical, chemical and electrochemical aspects. Anion exchange membrane electrolysers are at earlier stages of development: they are produced and commercialised, but still at a small scale. In 2030, according to [8], 84% of electrolyser capacity is presumed to be alkaline electrolysers (AEL), and 14% proton-exchange membrane electrolysers (PEM). The remaining 2% is expected to be solid oxide electrolysers (SOEC). Table 2.1 presents key characteristics of AEL, PEM and SOEC.

The cost of an installed electrolyser system can be divided into three main components: the stack, the balance of plant and the installation cost. The stack cost represents about 50-60% of the uninstalled electrolyser system, with the rest being the power supply unit (including the rectifier), oxygen separator tank, circulation pumps, piping, cooling system, valves, piping and various instrumentation, which is usually referred to as the balance of plant (BoP) [9]. Based on the capacity increase projections by announced projects, mass production and economies of scale, in particular to the stack, could lead to a decrease in the capital cost of an installed electrolyser system, with costs declining by 30% by the end of the decade according to the IEA [10].

The lower heating value (LHV) describes the energy content in hydrogen, excluding the latent energy content in the steam, which is released in combustion. The LHV efficiency represents the electrolyser's ability to convert electrical energy into hydrogen and is typically used when focusing solely on hydrogen production. Whereas, the higher heating value (HHV) includes the latent energy content. It is an important parameter when utilising the excess heat from a process because it reflects the total energy needed for hydrogen production, and the portion available as heat.

The operating temperature of an electrolyser impacts the potential for waste heat recovery. The alkaline (AEL) and proton exchange membrane (PEM) electrolysis is supplied by feeding liquid water and operating at temperatures usually below 100°C (50–80°C for PEM, 60-90°C for AEL [8]). Due to the low temperature levels, options for waste heat recovery are limited. Taking additional losses of heat transfer and transportation into account, spatially close applications and direct integration are considered to be the preferred options. Compared to low-temperature, high-temperature electrolysis, such as SOEC, can be supplied with steam and thus reducing the total energy demand by the heat of evaporation. However, typical operating temperatures of 650–900 °C are significantly above common DH temperature levels and partly contradict the intentions towards lower heat supply temperatures.

AEL has been commercially available since the early 1900s, offering a long lifespan and low investment costs (275-475 EUR/kW for year 2050 [6]) as it is often described to not rely on expensive, rare metals for production [11], which is assumed in this study. Instead, it utilises nickel alloys, as described in [12]. However, it can rely on rare metals such as ruthenium and iridium [13, 12]. AEL is primarily used by the fertiliser and chlorine industries and currently accounts for almost two-thirds of the global electrolyser capacity [11].

PEM has recently gained popularity, primarily due to its wider range of load flexibility (0-100%), and fast start-up times [11]. The production of PEM requires rare metals such as platinum and iridium, which results in a higher investment cost compared to AEL.

Solid oxide electrolysers (SOECs) achieve the highest efficiencies among electrolyser designs, although they need to use an external heat source for steam generation. SOECs are best placed where there is a heat source available (nuclear or industrial facilities). The SOEC technology is still at the demonstration stage and faces durability challenges, with a typical lifetime of around 2 years [14].

Table 2.1: Electrolyser properties.

	PEM	AEL	SOEC	Source
Operating temperature [°C]	50-80	60-90	650–900	[8]
Cold start-up time	5-10 min	1-2h	Hours	[8]
Load flexibility [%]	0-100	20-100	± 100	[8]
LHV efficiency [%]	66.4	69.9	72.5	[6]
HHV efficiency [%]	80.1	84.0	89.3	[6]
Investment cost [EUR/kW]	325-500	275-475	500-1100	[6]

Since AEL and PEM are the technologies currently dominating the market, they are selected as the electrolysers to investigate in this study. Moreover, the operating temperatures of these technologies are compatible for integration with the DH networks of cities in Northern Europe, as will be further discussed in this thesis.

2.2 Impacts of Integrating Electrolyser Waste Heat into District Heating Systems

The interplay between the hydrogen production process via electrolysis and district heating, as well as the potential heat integration between the two, has been investigated in some studies.

Bohm et al. [8] investigated the utilisation of waste heat from electrolysers in a DH system in Austria. They found that it is feasible by 2030 to cover about 12% of the current DH demand in Austria by waste heat recovery from electrolysers. However, they concluded that the operation of this heat source has a high dependency on the electricity market. As temperatures drop, heat demand rises, and electricity prices often follow the same trend. Electrolyser operation, however, is primarily driven by hydrogen demand, storage capacity, and electricity prices. According to Bohm et al., flexible production schedules may be completely misaligned with heat demand, as hydrogen could be produced when heat is least needed. Conversely, continuous hydrogen production would ensure a steady heat supply, but may still not coincide with the heat demand in the DH network.

A techno-economic evaluation of WHR from an off-grid alkaline water electrolysis plant supplying heat to a Finnish city was conducted by Meriläinen et al. [15]. The study investigated the optimal dimensioning of the WHR system to minimise the levelised cost of heat. The system included a pit thermal energy storage unit connected to a heat pump (HP) and an electric boiler (EB), as well as a separate HP for direct heat supply. It was found that the EB had no or very low investment in the cost-optimal solution, while HPs accounted for the largest single cost within the WHR system. The analysis is limited to an electrolysis waste heat temperature of 70°C.

Van der Roest et al. [16] examined different WHR system configurations for a PEM electrolyser with a waste heat temperature of 57°C. Both heat exchangers (HX) and HP for WHR were considered in the process. It was found that utilising waste heat from hydrogen production could increase the electrolyser's overall efficiency by around 15%. The study also showed that heat utilisation is sensitive to the transport distance. Recovering waste heat with HP is challenging compared to HX due to the higher cost of installation and operation. However, the analysis only considers the value for heat without including the value of hydrogen.

Jin et al. [17] investigated thermal management and heat recovery for low-temperature electrolysers, considering both system safety in the electrolyser as well as operating the electrolyser at a high efficiency. The analysis showed that approximately 20% of the input energy is released as excess heat when producing hydrogen with a low-temperature electrolyser. The use of HX and HPs was used for the integration of waste heat from electrolysers to DH networks. The waste heat temperature was assumed to be 79–80°C, with a DH supply temperature starting at 74°C. It was found that effective heat recovery improved overall efficiency from the power to the

hydrogen process by around 15%. This also improves the market competitiveness of green hydrogen produced from renewable energy. Despite the promising potential, the authors noted that challenges remain in thermal management and real-world system design to fully realise the benefits of heat recovery in electrolysis systems.

Frassl et al. [18] studied the technical and economic potential of waste heat recovery from AEL operating at 80°C and powered by excess renewable energy by using a simulation model for renewable power plants. The study examined the effects of heat utilisation from AEL in a DH system on economic viability, levelised cost of hydrogen, and system efficiency. The revenues from heat sales were included in the levelised cost of hydrogen, which resulted in hydrogen cost reduction during the hours when excess heat was recovered and sold. The results show that electrolyser efficiency, including hydrogen produced and heat supplied to the DH system, was 88.2% for small-scale electrolysers (i.e. 2.13 MW) and 82.3% for larger electrolysers (i.e. 6.39 MW). This can be compared to the maximum potential of energy, hydrogen and total waste heat, which was 89.4% for small-scale and 88.4% for larger electrolysers. The observed gap between the electrolyser sizes is primarily due to limited district heating demand, particularly during the summer months. Challenges related to the electrolyser's cooling strategy were identified, including oscillations in the cooling system under variable and partial load conditions.

The main findings of previous studies on WHR from electrolysers can be summarised as follows: (i) recovery and utilisation of waste from hydrogen production leads to an increase in the overall energy efficiency of the electrolyser, and (ii) reduction of the costs of heat and hydrogen.

There are no published studies that account for variations in heat and hydrogen costs across different electrolyser types with various waste heat temperatures integrated with WHR and connected to the DH system. To fill this gap, we apply a linear cost minimisation model using a Swedish city energy system to analyse the effects of integrating an electrolyser WHR process, taking into consideration the various possible electrolyser installations.

2.3 Waste Heat Recovery potential

As was mentioned in Section 2.1, the potential of heat recovery from an electrolyser mainly depends on the underlying technology and mode of operation, which define temperature levels of waste heat. Figure 2.1 shows potentials for heat recovery from AEL (a) and PEM (b) electrolysers. E_{ref} represents the electrical energy input needed per Nm^3 hydrogen at the average waste heat temperature for the type of electrolyser.

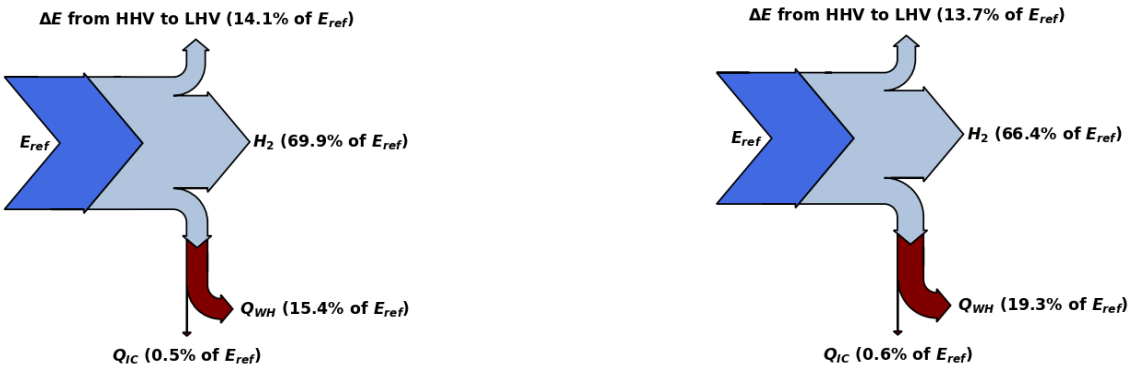

(a) (b)

Figure 2.1: Potentials for heat recovery from AEL at 75°C (a) and PEM electrolyser at 65°C (b).

Van der Roest et al. [16] investigated the integration of PEM electrolysers with district heating using both HX and HP. They found that heat costs are lower for the case when heat is recovered from PEM electrolyser with HX in comparison to HP due to the higher investment costs and operating costs of HP. Heat recovery from electrolysers with HP allows for a broader range of waste heat temperatures and can adjust the temperature lift to match the district heating supply. The waste heat temperature from low-temperature electrolysers ranges between 50-90°C. The waste heat from a PEM does not exceed 80°C, while the waste heat from an AEL does not fall below 60°C. The choice of heat recovery unit depends on the temperatures of both the heat source and the heat sink. For the case when the electrolyser‘s waste heat temperature (T_{WH}) is higher than the district heating supply temperature (T_{DH}), also when accounting for the temperature drop over the HX ($T_{DH} + \Delta T_{HX}$), only HX can be used as the heat recovery unit, see Equation 2.1. The district heating supply temperature typically ranges from 80 to 96°C.

$$T_{WH} > T_{DH} + \Delta T_{HX} \tag{2.1}$$

HP is used as a heat recovery unit in cases where the DH supply temperature is higher than the electrolyser´s waste heat temperature, see Equation 2.2.

$$T_{WH} < T_{DH} \tag{2.2}$$

A HP utilises the excess heat from the electrolyser to evaporate a refrigerant. The refrigerant is then compressed isotropically, raising its temperature through mechanical work. The heat is then transferred to the DH supply via the condenser, making

use of the recovered energy. HX has a low investment cost compared to HP. HP consumes electricity to produce heat, its running cost is related to the electricity price. Figure 2.2 shows possible configurations for waste heat recovery from the electrolyser with HX (a) and HP (b) as the heat recovery units.

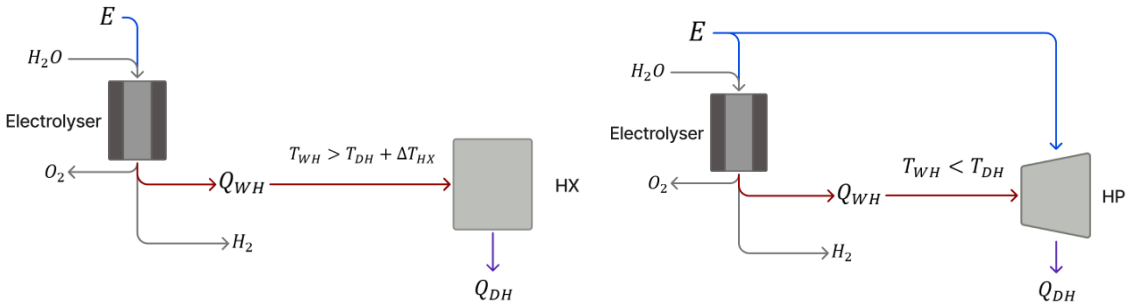

(a) **(b)**

Figure 2.2: Possible configurations for heat recovery from electrolyser with HX (a) and HP (b) as heat recovery units. E represents electricity demand for electrolyser and WHR unit, H_2O, O_2 and H_2 are water, oxygen and hydrogen, respectively. The heat from the electrolyser is denoted as Q_{WH}, and the heat delivered to the DH grid by Q_{DH}.

The coefficient of performance (COP) of HP is affected by the waste heat temperature. A smaller temperature difference between the waste heat and the DH supply leads to a higher theoretical maximum COP, see Equation 2.3.

$$COP_{carnot} = \frac{T_{DH}}{T_{DH} - T_{WH}} \tag{2.3}$$

The waste heat temperature further influences the efficiency properties of the waste heat recovery process. Within the electrolyser stack, the efficiency of hydrogen production is affected. Higher operating temperature corresponds to a reduction in cell voltage and specific energy consumption, and therefore a higher LHV efficiency [19]. For both PEM and AEL, increased temperature reduces specific energy consumption (γ) by 0.02–0.24 kWh/Nm^3/10°C. The reduction was assumed to be at the lower end of the range to avoid overestimating its impact, and the collected LHV efficiency [6] was assumed to be for the average temperature of the electrolyser type. The HHV-based efficiency increases proportionally with the LHV-based efficiency, following the ratio between the higher and lower heating values of hydrogen [19]. Equations 2.4 and 2.5 display the calculation of these efficiencies.

$$\eta_{LHV} = \frac{LHV_{H2}}{E_{ref} - \frac{\gamma}{10} \cdot (T_{WH} - T_{WH,ref})} \tag{2.4}$$

$$\eta_{HHV} = \eta_{LHV} \cdot \frac{HHV_{H2}}{LHV_{H2}} \tag{2.5}$$

Waste heat efficiency (η_{WH}) is defined as the ratio of waste heat that is generated per electrical input in the electrolyser, and is calculated as in Equation 2.6. The thermal energy lost in the internal cooling system is represented as η_{IC}.

$$\eta_{WH} = (1 - \eta_{HHV}) \cdot \eta_{IC} \tag{2.6}$$

Figure 2.3 shows LHV (a), HHV (b) and waste heat efficiency (c) for PEM and EAL electrolysers for waste heat temperature range of 50 to 90°C. It was assumed that 3% of the heat is lost internally [6] and the factor for reduced energy consumption is 0.03 kWh/Nm^3/10°C [19].

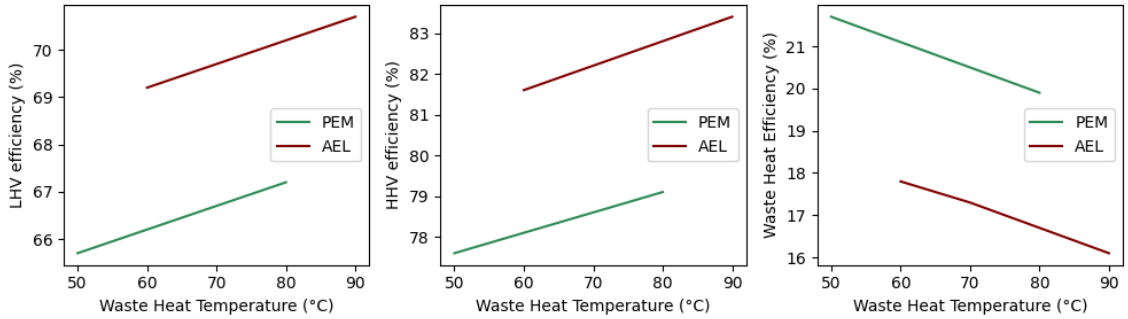

Figure 2.3: LHV (a), HHV (b) and waste heat efficiency (c) for PEM and EAL electrolysers for waste heat temperature range of 50 to 90°C.

AEL output can fluctuate within the operational range of full capacity to 20% of full capacity, while PEM electrolyser can be stopped and started relatively rapidly, i.e., operational range of 0-100% [8]. Table 2.2 describes configurations for waste heat recovery from electrolysers investigated in this work. Waste heat temperatures ranging from 50 to 90°C are analysed. Evaluating WHR system performance across the full temperature range allows for assessing the cost-effectiveness and performance (i.e., hydrogen and heat production) of different configurations. It should be noted that only one configuration corresponds to the conditions under which HX can be used for recovery, seen in Equation 2.1.

Table 2.2: Configuration options for WHR process

Configuration	Electrolyser type	WHR Unit	T_{WH}[°C]	η_{LHV} [%]	η_{WH} [%]
AEL90	AEL	HX	90	70.6	15.8
AEL90(HP)	AEL	HP	90	70.6	15.8
AEL80	AEL	HP	80	70.1	16.5
AEL70	AEL	HP	70	69.7	17.2
AEL60	AEL	HP	60	69.2	17.8
PEM80	PEM	HP	80	67.1	20.0
PEM70	PEM	HP	70	66.6	20.6
PEM60	PEM	HP	60	66.2	21.1
PEM50	PEM	HP	50	65.7	21.7

3
Background

This chapter provides an overview of Gothenburg's current waste heat and hydrogen production, along with future perspectives in these areas. The current status and future projections of waste heat production are also outlined, with particular focus on the integration of industrial excess heat. Finally, the chapter discusses hydrogen production in the city, focusing on the transition from fossil-based methods to electrolysis within the refinery sector, and how this shift increases the availability of waste heat.

3.1 Waste heat - current status and future perspectives

Over the past few decades, the development of district heating networks in Sweden has played a major role in lowering CO_2 emissions from the heating sector, as described by Werner et al. [20]. A significant part of this reduction comes from the integration of industrial excess heat into these systems. Because the emissions associated with this heat are usually attributed to the primary industrial products, its use in district heating is generally seen as emissions-free. However, there is ongoing debate whether such heat should be classified as CO_2-free or merely CO_2-neutral, as highlighted by Pelda et al. [21]. In Gothenburg, approximately 70% of the heat supplied to households today comes from recovered sources [22], including the ST1 and Preem refineries and the Renova waste-to-energy CHP plant.

The Renova waste-to-energy (WtE) plant is located in Sävenäs and handles combustible waste, mostly from municipalities in the Gothenburg region, but also imports waste from other regions in Sweden and Europe [23]. The waste primarily consists of municipal solid waste (MSW). 550 000 tonnes of waste is burned each year, and the Sävenäs plant supplies a third of the heat in the Gothenburg DH grid and 5% of the electricity demand. Regarding the future operation of the plant, Renova states that they prepare for the future by at least 30 years [24]. While waste generation is decreasing, the growing population in the area suggests that waste levels will remain steady.

Plastic usage has increased in Sweden by almost 30 kg per person and year from 2010 to 2017, which also leads to more plastic waste according to the Swedish Environmental Protection Agency[25]. Most of the plastic waste is used for energy recovery or fuel within the industry, and only about 10% is recycled. The plastic content in the MSW stands for 40% of the carbon emissions from the WtE plant according to Renova[23]. To address carbon emissions, strategies such as carbon capture and storage (CCS) or carbon capture and utilisation (CCU) are considered, where CCS aims to reduce emissions by storing CO_2, while CCU focuses on making better use of the captured carbon. In 2024, a decision in principle was made to implement this on one of the four waste lines until 2030. In that case, around 100 000 tonnes of carbon dioxide can be captured [24]. Deploying CCS or CCU requires additional electrical energy, 73.99 kWh per tCO_2 mitigated, according to Van der Meer [26].

There is a growing demand in the market for plastics derived from non-fossil feedstocks. The chemical industry in Stenugnsund needs this type of feedstock in order to reach its sustainability vision for 2030 [27]. Plastic that cannot be recycled mechanically can be processed in a plastic recycling refinery, thereby avoiding incineration and the associated carbon emissions. Furthermore, there are additional initiatives aimed at reducing plastic usage and waste, such as replacing plastic with alternative materials, extending its lifespan, avoiding single-use applications, and promoting reuse for as long as possible [28]. It is estimated that 58% of MSW consists of plastic [27]. Removing this plastic would result in a lower heating value for the waste, which would, in turn, affect both electricity and heat generation at the WtE plant. In equations 3.1-3.4, the heating value for waste with and without plastic is calculated. The parameters used in the equation were found through Renova's 2024 sustainability report [29].

$$LHV_{\mathrm{w1}} = \frac{E_{\mathrm{e}} + E_{\mathrm{h}}}{m_{\mathrm{w}}} = 12.134 \text{ MJ/kg} \tag{3.1}$$

$$m_C = m_{CO_2} \cdot \frac{12}{44} \tag{3.2}$$

$$E_{\mathrm{p}} = m_C \cdot f_{\mathrm{p}} \cdot LHV_{C,\mathrm{p}} = 802,076 \text{ MWh} \tag{3.3}$$

$$LHV_{\mathrm{w2}} = \frac{E_{\mathrm{e}} + E_{\mathrm{h}} - E_{\mathrm{p}}}{m_{\mathrm{w}}} = 6.884 \text{ MJ/kg} \tag{3.4}$$

3.2 Hydrogen production - status and future perspectives

Sweden's oil refinery sector is responsible for about 5% of the country's total greenhouse gas (GHG) emissions [30]. The majority of these emissions, around 70%, are linked to energy use during refining processes, while the rest mainly result from hydrogen production using natural gas. The industry is dominated by three companies: Preem, St1, and Nynäs. The primary refinery sites are concentrated in Västra Götaland (Preem and St1) and the Stockholm area (Nynäs). Preem is the largest actor, operating two major fuel refineries in Lysekil and Gothenburg. Together, these facilities account for 80% of Sweden's total refining capacity and roughly 30% of the refining capacity in the Nordic region [31]. St1, which also focuses on fuel production, runs a refinery in Gothenburg. In West Sweden, the installed capacity for hydrogen production amounted to 760 MW in 2022 [32]. Half of the hydrogen production capacity is produced as a byproduct of other processes. The other half is produced by steam methane reforming (SMR), using natural gas [32].

Gothenburg City's energy plan for 2022-2030 aims to meet the environmental goals of reducing energy use of buildings, only producing energy from renewable sources and reducing the climate impact of the transport sector [22]. This plan outlines possibilities for future hydrogen utilisation within the city, such as its use for energy storage to balance renewable energy production, as fuel for the city's vehicle fleet, fuel for thermal generation, and for producing biofuels in refineries. Two key ways for CO_2 emissions reduction from hydrogen production are presented in the plan: hydrogen production from natural gas through the SMR process combined with CCS, and hydrogen production through electrolysis.

CCS technology can utilise considerable amounts of industrial excess heat. Eliasson et al. [33] investigated the impacts of the recovery of available excess heat from the refinery plant to drive the CCS capture unit on the cost of the CCS and district heating network. They found that for the case where CCS is prioritised for the use of excess heat over district heating, the capture cost results in 27 EUR/tCO_2 , while in the case where maintaining the amount of district heating supplied is prioritised, the cost is 40 EUR/tCO_2. It should be noted that if excess heat at the industrial plant is utilised by CCS technology, less heat could be available for district heating, potentially reducing the supply to the network. This could lead to higher heating costs. Implementing CCS on existing SMR would reduce carbon emissions [32].

Renewable hydrogen, as defined by the EU, must come from non-biological sources [34]. This means that the possibility for member states to provide support for biogenic hydrogen is limited and indicates that it is not perceived by lawmakers as an important part of the future hydrogen supply. Electrolysis uses electricity and water to produce hydrogen gas, oxygen gas and residual heat. The electrolysis process has no direct emissions, but does require electricity, ca. 1.5 units of electricity per unit of produced hydrogen [6]. In Gothenburg, both Preem and St1 are currently investigating the potential of implementing green hydrogen production [31, 35]. If refineries in Västra Götaland were to fully transition their current fuel production, from utilising hydrogen from SMR to electrolysers, the resulting hydrogen demand would amount to 14 TWh annually [32]. The estimated share of demand for Gothenburg in this scenario is 5 TWh/year, derived from Rosén et al. [36]. This would require ca. 7.6 TWh of electricity, i.e. 34% of the current (2024) Gothenburg electricity demand [37]. The production of 5 TWh of hydrogen via AEL/PEM electrolyser allows to utilise ca. 1.4 TWh of the excess heat per year. This heat would also be produced in addition to pre-existing levels of waste heat generation from the refineries. The SMR units currently used for hydrogen production are endothermic, meaning they require heat to operate [38]. Therefore, waste heat recovery from electrolysers within refineries (Preem and St1) would increase the amount of excess heat currently produced since electrolysers are exothermic and are direct replacements for the SMR units. However, a combination of decreased production levels and processed raw materials would lead to a lower hydrogen demand for the refineries in Västra Götaland, estimated to 4.9 TWh/year [32]. Based on the distribution in [36], this would amount to 1.7 TWh/year in Gothenburg.

4

Methodology

A linear cost minimisation model was applied to investigate the potential and implications of integrating waste heat from electrolysers into the existing DH network in Gothenburg. The model was originally developed by Heinisch et al. [39] to study the interconnection between the electricity and heating sectors in cities. Bertilsson et al. [40] further developed this model to study how different properties of cities, such as the city's electricity import capacity and the size of industry- and transport sectors, impact energy system composition, i.e, heat and electricity generation and capacity. Yu et al. [41] included the physical properties of the DH grid into the model to analyse the losses and bottlenecks associated with the transmission of heat in DH grids. The model applied in this work has been further extended to include the electrolysers and accompanying WHR units described in Section 2.3. The model minimises the total system cost and is constrained to produce zero net emissions for the Year 2050 with an hourly resolution.

The city of Gothenburg and Mölndal municipality are divided into seven heat regions in this study, see Figure 4.1 (left). This reflects the allocation of DH production units across the city and aligns the district division in the program Göteborg Energi uses [42]. The lines within the heat region indicate possible pathways for heat transmission between regions. By modelling this spatial representation, heat transmission between regions is limited by DH grid capacity within the city. Figure 4.1 (right) shows the four electricity regions modelled in this thesis. Each region has a specific electricity import capacity from outside the geographical boundaries of the modelled system, whose prices are described in Section 4.2.2. Each region further has separate electricity demand profiles, representing demand for all hours of the year. In addition, both electricity-consuming and generating technologies are invested in these regions as added demand or generation, respectively.

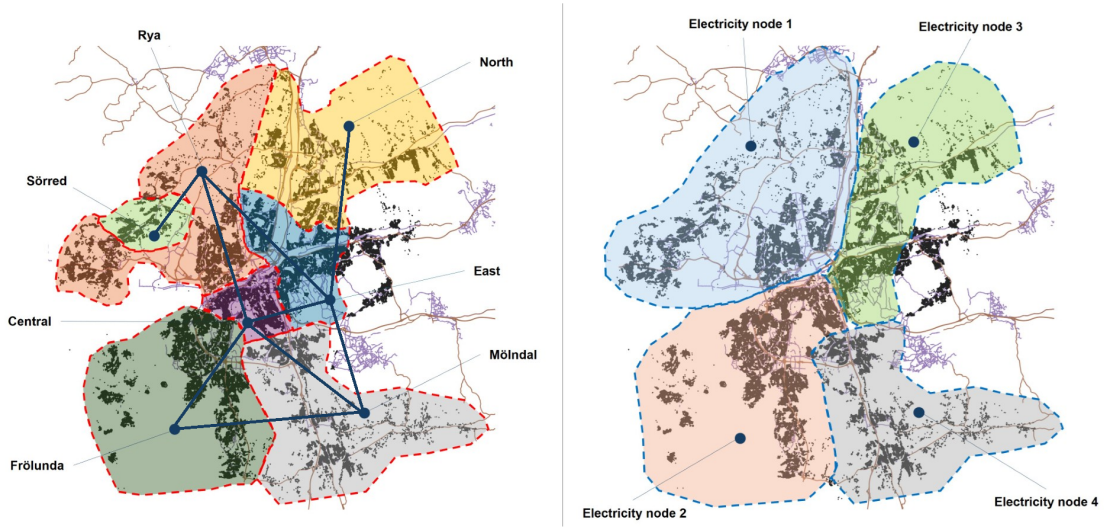

Figure 4.1: Seven heat regions (left) and four electricity regions (right).

Electricity and heat regions may coincide geographically. In such cases, a CHP plant can, for example, deliver heat to the heat region and supply electricity to the corresponding electricity region. These overlaps are indicated with a mark in Table 4.1.

Table 4.1: The overlapping of heat regions with electricity regions represented along the top row and heat regions listed in the first column.

	E1	E2	E3	E4
Central		✓	✓	
East	✓		✓	
Frölunda		✓		
Mölndal				✓
North	✓		✓	
Rya	✓			
Sörred	✓			

The composition of future heating units remains uncertain; however, some units are currently under construction or have been recently commissioned. The units assumed to be remaining in the system by 2050 are listed in Table 4.2. Additionally, a thermal energy storage (TES) facility with a capacity of 1 GWh has been in place in the East region since 2018 [43].

Table 4.2: Preexisting heat regions and heat generation units within.

Regions	Plants	Waste heat
Central		
East		Renova
Frölunda	Biomass-fuelled HOB	
Mölndal		
North		
Rya	Biomass-fuelled HOB , Biomass-fuelled CHP, Industrial HP	Preem, ST1
Sörred		

For other types of electricity and heat generation technologies and storage, the model is formulated as a greenfield. Thus, no pre-existing production technologies or storage systems for heat and electricity are assumed to be in place, and all investment decisions are made based on the energy demands of the modelled year.

4.1 Model description

Equation 4.1 describes the model's objective function, which is to minimise the total investments and running costs of Gothenburg's energy system. A full list of symbol definitions is found in the nomenclature of this thesis.

$$\begin{aligned}\min\ C^{tot} = &\sum_{i\in I}\sum_{e\in E}\left(C_i^{inv}+C_i^{OM_{fix}}\right)\cdot s_{i,e}+\sum_{i\in I}\sum_{h\in H}\left(C_i^{inv}+C_i^{OM_{fix}}\right)\cdot s_{i,h}\\ &+\sum_{i\in I}\sum_{e\in E}\sum_{t\in T}C_i^{run}\cdot p_{i,e,t}+\sum_{i\in I}\sum_{h\in H}\sum_{t\in T}C_i^{run}\cdot q_{i,h,t}\\ &+\sum_{i\in I}\sum_{t\in T}\left(c_{i,t}^{start}+c_{i,t}^{part_{load}}\right)\\ &+\sum_{e\in E}\sum_{t\in T}C_t^{imp}\cdot w_{e,t}^{imp}\end{aligned} \tag{4.1}$$

The function minimizes total annual costs (C^{tot}) which is equal to the investment cost (C_i^{inv}), fixed operations and maintenance costs ($C_i^{OM_{fix}}$) and the running cost (C_i^{run}) of each technology i. Start-up ($c_{i,t}^{start}$) and part-load cost($c_{i,t}^{part_{load}}$) were implemented for thermal generation technologies to represent cycling properties of these technologies. The modelling approach, which represents flexibility-related properties of thermal generation, is based on the two-variable approach described in [44]. Here, $s_{i,e}$ and $s_{i,h}$ denote the installed capacity of a certain technology i in electricity region e and heat region h, respectively. The variables $p_{i,e,t}$ and $q_{i,h,t}$ represent the power output and heat output of a certain technology i in electricity region e and heat region h at time-step t, respectively. The variable $w_{e,t}^{imp}$ denotes the imported amount of electricity to electricity region e at time-step t.

The electricity demand must be satisfied for each time-step and electricity region, which necessitates Equation 4.2.

$$D^{el}_{e,t} + \sum_{h \in e} \left(\sum_{i \in I_{pth}} \left(\frac{q_{i,h,t}}{\eta_i} \right) + H2^{el}_{h,t} \right) + b^{ch}_{e,t} \leq \sum_{h \in e} \left(\sum_{i \in I_{CHP}} p_{i,h,t} \right) + \sum_{i \in I_{el}} p_{i,e,t} + b^{dch}_{e,t} + w^{imp}_{e,t}, \quad \forall\, e \in E,\ \forall\, t \in T \tag{4.2}$$

The left-hand side of this equation is the sum of the assumed demand inputs for each time-step t and electricity region e: hourly electricity demand ($D^{el}_{e,t}$); the electricity for power-to-heat (calculated as the heat produced divided by the technology efficiency, $\frac{q_{i,h,t}}{\eta_i}$); the electricity demand from electrolysers $H2^{el}_{h,t}$; and charging of stationary batteries ($b^{ch}_{e,t}$). These demands must, in all regions e and all time-steps t be less than or equal to the electricity generatated from CHP plants($\sum_{i \in I_{CHP}} p_{i,h,t}$) summed over heat regions h that overlap with the electricity region e; the electricity generated ($p_{i,e,t}$) from power generating technologies (I_{el}); the discharge of electricity from stationary batteries ($b^{dch}_{e,t}$); and the import of electricity from outside the system $w^{imp}_{e,t}$.

The heating demand must be met at every hour of the year and must be produced by technologies within the city. Equation 4.3 defines the heat balance for each heat region $h \in H$ and time-step $t \in T$.

$$D^{heat}_{h,t} + \sum_{i \in I_{TES}} TES^{ch}_{i,h,t} - HP^{heat,\ ind}_{h,t} \leq \sum_{i \in I_h} q_{i,h,t} + \sum_{i \in I_{TES}} TES^{dch}_{i,h,t} \quad \forall\, h \in H,\ \forall\, t \in T \tag{4.3}$$

On the left-hand side, the total heat demand consists of: the specific heating demand $D^{heat}_{h,t}$; the heat charged to thermal energy storage units $TES^{ch}_{i,h,t}$ (for all TES technologies I_{TES}); and the reduction in DH demand due to the use of individual heat pumps, denoted by $HP^{heat,\ ind}_{h,t}$. This total demand must, in all regions h and time-steps t, not exceed the heat supply, shown on the right-hand side, The supply includes: heat generation $q_{i,h,t}$ from all heating technologies I_h within the region; and the heat discharged from thermal energy storage units $TES^{dch}_{i,h,t}$.

The constraints which are applied to represent WHR from electrolysers in the model, as well as a description of their functions, can be seen in Table 4.3. Additional constraints applied in the model can be found in Appendix A, Table A.1.

Table 4.3: Constraints to represent WHR from electrolysers in the model

Constraints	**Description of constraints**
Storage level, H_2	The H_2 storage level $SOC^{H_2}_{h,t}$ per heat region h at time-step t cannot exceed the H_2 storage level $SOC^{H_2}_{h,t-1}$ at the previous time-step plus H_2 generation $H2^{gen}_{i,h,t}$ minus hydrogen demand $D^{H_2}_{h,t}$ $$SOC^{H_2}_{h,t} \leq SOC^{h_2}_{h,t-1} + \sum_{i \in I_{elec}} H2^{gen}_{i,h,t} - D^{H_2}_{h,t}$$ $$\forall\ h \in H, \forall\ t \in T$$
Maximum storage, H_2	The H_2 storage level $SOC^{H_2}_{h,t}$ per heat region h at time t cannot exceed the capacity $s_{h_2,h}$ of the H_2 storage. $$SOC^{H_2}_{h,t} \leq s_{h_2,h}$$ $$\forall\ h \in H, \forall\ t \in T$$
Maximum production, H_2	The production of H_2 cannot exceed the installed capacity of the electrolyser. $$H2^{gen}_{i,h,t} \leq s_{i,h}$$ $$\forall\ i \in I_{elec}, \forall\ h \in H, \forall\ t \in T$$
Minimum production, $H_{2,\ AEL}$	AEL electrolysers cannot operate below 20% load capacity. (see Table 2.1 for details.) $$H2^{gen}_{i,h,t} \geq 0.2 * s_{i,h}$$ $$\forall\ i \in I_{elec,\ AEL}, \forall\ h \in H, \forall\ t \in T$$
Maximum production, WHR	The heat produced from WHR units is less than the useful heat produced from its electrolyser. $$\sum_{i \in I_{HP,WHR}} q_{i,h,t} + \sum_{i \in I_{HX,WHR}} q_{i,h,t} \leq H2^{gen}_{i,h,t} * \eta^{WHR}_i$$ $$\forall\ h \in H, \forall\ t \in T$$
Maximum production, WHR_{HP}	WHR HP units can only operate when DH temperature is low enough. $$\sum_{i \in I_{HP,WHR}} q_{i,h,t} \leq H2^{gen}_{i,h,t} * \eta^{WHR}_i * P_{HP,\ WHR}$$ $$\forall\ h \in H, \forall\ t \in T$$
Maximum production, WHR_{HX}	WHR HX units can only operate when DH temperature is high enough. $$\sum_{i \in I_{HX,WHR}} q_{i,h,t} \leq H2^{gen}_{i,h,t} * \eta^{WHR}_i * P_{HX,\ WHR}$$ $$\forall\ h \in H, \forall\ t \in T$$

4.1.1 WHR availability profiles

As mentioned in Section 2.3, eight electrolysers were added to the model, chosen from both types of electrolysers, PEM and AEL, and chosen to span the temperature range.

To retain a linear programming formulation, several simplifications were made when estimating the HX availability and the COP for HPs. Both parameters are influenced by the DH supply temperature, which plays a central role in the model. Capturing the thermodynamic properties causing limitations in the availability of WHR units, described in Section 2.3, would introduce non-linearities: HX availability would require binary variables to model on/off behaviour based on temperature thresholds, and the COP expression involves division by a variable. These elements would violate the linearity requirements of the LP model and complicate the solution process. To maintain linearity, DH supply temperatures from a reference model were instead used to generate fixed hourly profiles for both HX availability and HP COPs. The maximum COP was capped in accordance with [15]. Although this breaks the feedback loop between heat production and DH temperature, it enables consistent representation of waste heat recovery options while ensuring computational efficiency. This trade-off supports the analysis of larger system-level interactions without compromising solvability.

4.2 Data

The techno-economic data for investments and running costs for the available production and storage technologies are collected from DEA [45]. The estimated control values for the year 2050 for costs and lifetime have been used. The costs and lifetime for the HP used for electrolyser WHR were also collected from DEA [45], but HX costs were calculated as described in Section 4.2.1.

4.2.1 HX cost calculation

The required data for modelling HX used in the WHR system were the cost per unit of transferred heat and the temperature drop over the HX. The temperature drop was estimated to be 3°C as stated by Van der Roest [16]. The cost of heat exchangers can vary depending on several different factors in the design process of the technology. This means that an established universal value for the cost of heat exchangers is hard to estimate. Consequently, this provided an incentive to calculate an estimate of the HX cost based on the known design parameters in the WHR system. Equation 4.4 shows how the required heat transfer area was calculated. Since the annual demand of hydrogen was known, the annual amount of usable heat (Q $[W]$) could be estimated based on the electrolyser HHV and LHV efficiencies. Furthermore, the overall heat transfer coefficient (U) was estimated to be 1200 $[W/m^2]$ because of water-to-water heat transfer. The mean logarithmic temperature difference (ΔT_{lm} [°C]) was calculated based on known temperatures on the DH side and required temperatures in the electrolyser to enable usage of HX.

$$A_{WHR} = \frac{Q}{U\Delta T_{lm}} \qquad \text{where} \qquad \Delta T_{lm} = \frac{(T_1 - t_2) - (T_2 - t_1)}{ln\frac{(T_1 - t_2)}{(T_2 - t_1)}} \tag{4.4}$$

The cost estimation per heat transfer area for shell and tube heat exchangers was taken from Ulrich and Vasudevan [46]. The cost of a shell and tube HX ($C_{HX,\ table}$[\$]) is \$ 85,000 if the heat transfer area ($A_{table}[m^2]$) is 1000 m^2. Using equation 4.5, the total cost of installing the required heat transfer area for the HX in the WHR system could be calculated. The exponent a was set as 0.6 as stated in [46]. Lastly, the cost per heat transfer capacity (C_{HX} [EUR/kW]) was calculated using equation 4.6.

$$C_{HX,\ tot} = C_{HX\ table}(\frac{A_{WHR}}{A_{table}})^a \tag{4.5}$$

$$C_{HX} = \mathrm{C}^{\mathrm{rate}}_{\mathrm{USD,\ EUR}} * \frac{C_{HX,\ tot}}{Q * 10^{-3}} \tag{4.6}$$

4.2.2 Electricity spot price

The annual spot price of electricity, used in the model to depict Year 2050, is derived from Göransson et al. [47]. This electricity price reflects conditions in Sweden's SE3 electricity region in 2050, under the scenario where no new nuclear power is required (although it is permitted from 2040), and investments in offshore wind are allowed along the entire Swedish coastline, including the southern Baltic Sea. The spot price is visualised in Figure 4.2

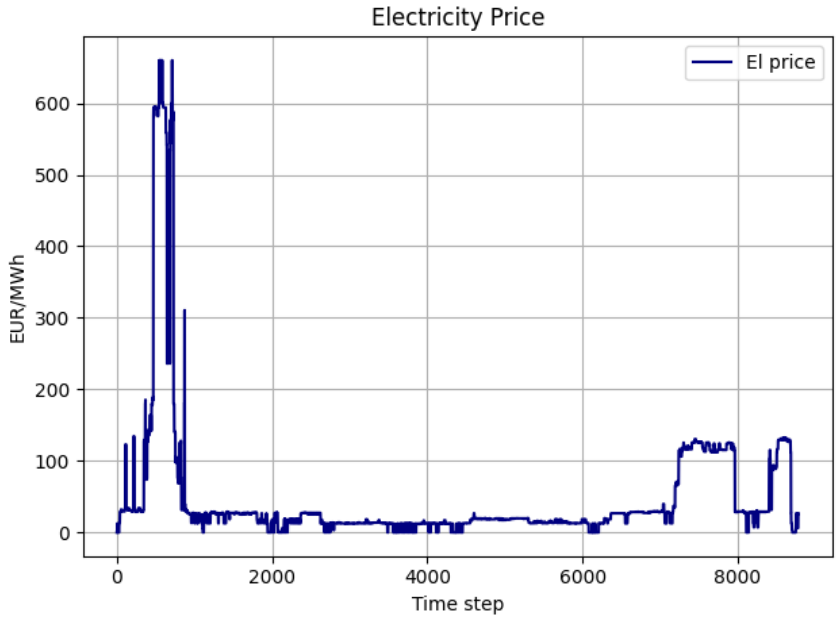

Figure 4.2: Electricity spot price.

4.2.3 Hydrogen Demand and Storage

The hydrogen demand in Gothenburg was based on the lower estimate of 1.7 TWh discussed in Section 3.2, and was allocated to the refineries located in the heat region Rya. It was assumed that the hydrogen demand was evenly distributed across all hours of the year to support continuous industrial processes. To meet the constant demand, the electrolysers must either produce hydrogen continuously at a constant rate or vary it's production with the help of a hydrogen storage. The hydrogen storage that is available for investments in the model is an LRC cavern.

The average annual marginal cost of hydrogen, used in the results as an indicator of the cost of hydrogen, was calculated according to equation 4.7.

$$\mathrm{MC}_{\mathrm{H_2}}^{\mathrm{avg}} = \frac{1}{8760} \sum_{t \in T} \left(\mathrm{MC}_t^{H_2 \ balance} \right) \tag{4.7}$$

4.2.4 Heat demand

The estimated demand for heat in Gothenburg 2050 that was used in the model was obtained from Statistics Sweden (Statistiska Centralbyrån) [48]. The temperature of the district heating supply is tied to demand, with increased load resulting in a higher supply temperature, see Figure 4.3. However, the supply stream temperature is also connected to the export and import of heat between regions, which is why it is not constant but variable in the model. Additionally, because the export of heat from one region to another takes time, depending on the velocity of the district heating flow and the distance between the exporting and importing regions, the heat must be produced before the actual increase in demand occurs.

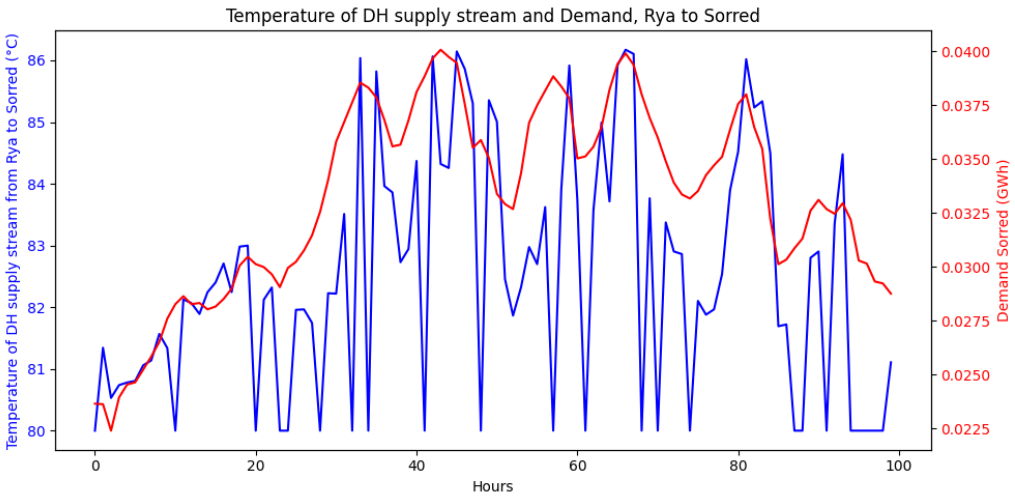

Figure 4.3: Representation of the relation between DH supply temperature and heat demand.

The average annual marginal cost of heat, used in the results as an indicator of the cost of heat, was calculated according to equation 4.8.

$$\mathrm{MC}_{\mathrm{heat}}^{\mathrm{avg}} = \frac{1}{7 \cdot 8760} \sum_{h \in H} \sum_{t \in T} \left(\mathrm{MC}_{h,t}^{\text{heat balance}} \right) \tag{4.8}$$

4.2.5 Industrial context of Gothenburg

In the industrial context of Gothenburg in 2050, it is assumed that the EU ETS emission cap has gradually decreased, leading to higher costs for emission allowances. This is expected to drive industries toward lower emissions. In this study, it was assumed that the refineries have reduced their fuel production as a result. In addition, it was assumed that all SMRs producing hydrogen for the refinery processes in Gothenburg will be replaced by electrolysers to reduce emissions. Consequently, since the demand for hydrogen will exist in conjunction with the refineries, the electrolysers in the model are limited geographically to where the refineries are located today.

The hydrogen demand is linked to the production level of the refineries, which in turn is tied to waste heat generation. The amount of available waste heat per unit of produced fuel, excluding heat from electrolysis, was assumed to remain at current levels. This is because SMR is not an exothermic process, and replacing SMR units with electrolysers, which are exothermic, increases the amount of heat produced in the refinery. The rest of the refinery process was assumed to generate the same amount of heat per unit of fuel as it does today. Refinery fuel production was assumed to drop to one-third of today's levels, to 940 GWh per year.

Furthermore, emissions from Gothenburg's municipal waste were assumed to be reduced by removing plastics and sending them to Stenungsund for recycling, as described in Section 3.1. Municipal solid waste levels are assumed to remain the same as today, which implies that excess heat from Renova decreases proportionally to the reduction in lower heating value (LHV) of waste when plastic is removed. This results in a heat production of 56.7% of the current heat production levels from Rya in 2050, to 433 GWh per year.

4.3 Investigated Scenarios

The scenarios investigated in this work can be divided into three main groups: reference cases (i); cases with varying electrolyser availability (ii); and sensitivity analysis. These are illustrated in Figure 4.4.

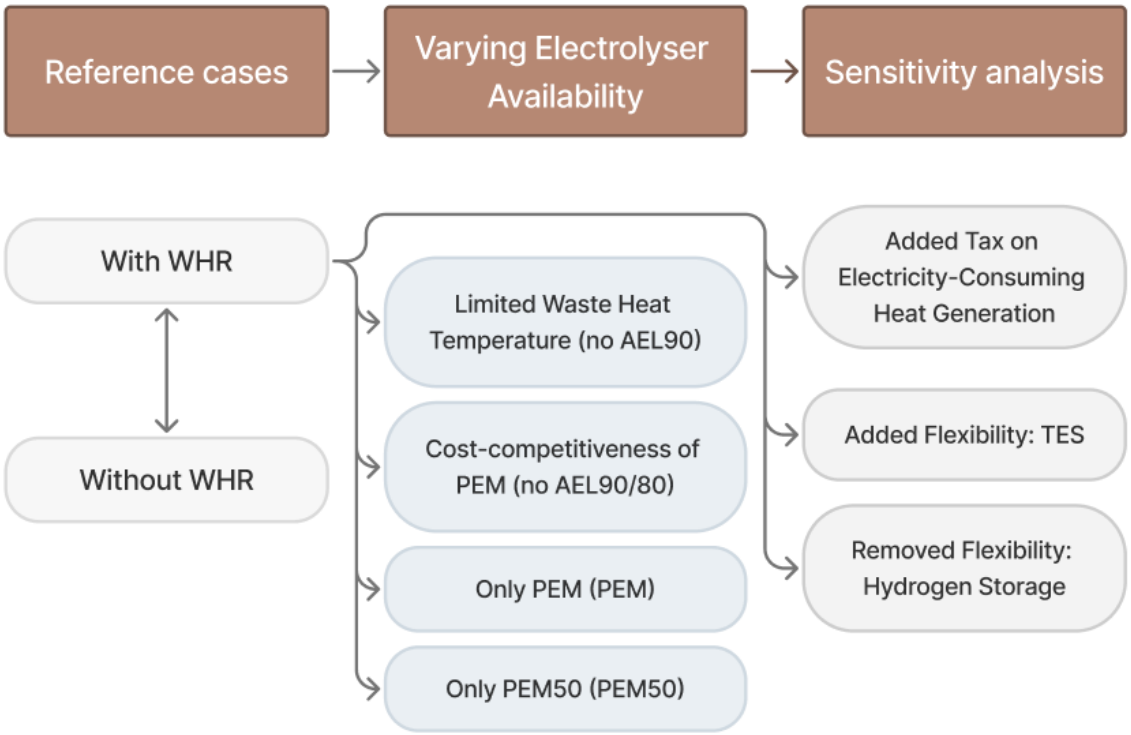

Figure 4.4: Visual representation of the scenarios explored in the model.

Two reference cases were investigated in this study; a system with and without access to WHR technology. The case *without WHR* represents the case when investments in a waste heat recovery system are not allowed in the model. The case *with WHR* represents a system in which investments in all nine WHR configurations described in Section 2.3 are allowed. The WHR configurations vary depending on electrolyser type, waste heat recovery unit and waste heat temperature. The aim of comparing these two reference cases, a system with and without access to WHR, was to answer the first research question; *What is the cost-optimal composition of the energy system in Gothenburg when integrating waste heat recovery from electrolysis?*

4.3.1 Varying Electrolyser Availability

To further analyse the results of the model, cases were constructed that limited the available electrolyser technologies, and thus WHR configurations, that the model could invest in. This was done to answer the second research question; *How does the choice of electrolyser influence the operation of heat and hydrogen generation, and what are the implications regarding the cost of heat and hydrogen?*

The combination of electrolysers and WHR units selected in the reference case *With WHR*, under full electrolyser availability, allows investments in all WHR configurations designed in this thesis, resulting in the most cost-effective model solution. To explore the impact on the system level caused by the choice of electrolyser, the model was adapted and compared to the cost-optimal combination. For each configuration, the total system cost, cost of hydrogen, and cost of heat are evaluated.

The following cases with limited availability of electrolysers were investigated:

Limited Waste Heat Temperature (no AEL90): Removing the option to invest in the AEL90 electrolyser excludes the configuration that provides the highest waste heat temperature, the only technology compatible with heat exchangers, and the highest hydrogen production efficiency. This case allows for analysis of the impact on the model results, i.e., total system cost, cost of hydrogen, and cost of heat, when the most cost-effective WHR configuration among all designed (see Table 2.2) is excluded.

Cost-competitiveness of PEM (no AEL90/80): Both AEL90 and AEL80 are excluded, which limits investments into WHR configurations based on low-temperature electrolysers, i.e, more expensive alternatives. This setup aims to investigate whether the model would invest in the most cost-efficient PEM electrolyser (PEM80) or opt for the third most cost-effective alkaline option (AEL70).

Only PEM (PEM): In this case, all AEL-type electrolysers were excluded, limiting investments to PEM electrolysers only. While PEM technologies have higher investment costs, they offer a more dynamic oporational performance.

Only PEM50 (PEM50): For this case, only PEM50 is available. It is the least efficient option (LHV and HHV), with the lowest waste heat temperature and has a high investment cost compared to AEL alternatives, but it offers better dynamic performance than AEL and is the electrolyser which produces the most waste heat per energy input. This case was constructed to investigate whether the model would invest in PEM50's corresponding WHR technology despite it being the least cost-effective option.

4.4 Sensitivity Analysis

The scenarios were constructed in order to test how sensitive the results from the reference cases are to changes in key input parameters and assumptions.

4.4.1 Tax on Electricity-Consuming Heat Generation

The impacts of tax on electricity-consuming heat generation technologies on the model results were investigated. Currently (2025), a tax of ca. 55 [EUR/MWh] is applied to PtH technologies [49] and could affect the results if still present in 2050. The objective function of the model (Equation 4.1) was thus adapted with the additional cost described in Equation 4.9.

$$\sum_{h \in H} \sum_{t \in T} \sum_{i \in I_{pth}} C_i^{tax} \cdot q_{i,h,t} \tag{4.9}$$

In this added cost, summed over all heat regions h, time-steps t, and PtH technologies I_{pth}, the tax (C_i^{tax}) was applied to the heat generation ($q_{i,h,t}$) of PtH technologies. Two versions of the tax were modelled, one where all PtH technologies were taxed equally, and one where the tax only applied to individual heat pumps. These cases, i.e., tax for all PtH technologies and tax for only for individual HP, investigate how a maintained tax level and a tax structure favouring DH would affect the system composition, respectively. While the tax has steadily increased in Sweden over the years [50], an assumption was made that the tax will be at similar levels in 2050 to avoid speculations in future policy decisions. These cases were selected based on relevant policy developments: in Sweden, the tax has been in place since 1951 [51], while Finland recently implemented a substantial tax reduction specifically for large-scale PtH technologies connected to district heating [52]. Given the potential for similar policy shifts in our region, these cases provide valuable insights into possible future scenarios

4.4.2 Investments in TES

Due to uncertainties about the future availability and potential placement of TES, its use was deliberately restricted in the reference case. This sensitivity analysis explored how a limited addition of tank-based TES could introduce some temporal flexibility between heat generation and demand, and how this might influence the energy system. Specifically, 1 GWh of tank TES was permitted in the heat region East, reflecting the current real-life setup [53], and up to 1 GWh of tank TES was allowed in Rya. This case aimed to represent a scenario aligned with today's storage levels and to explore the interaction between TES and the electrolyser's waste heat recovery (WHR) in Rya.

4.4.3 No Investments in Hydrogen Storage

There are uncertainties surrounding the technical feasibility of hydrogen storage at the scale required. According to Edvall [32], conditions for hydrogen storage using LRC in rock caverns in western Sweden are not known. The case without investments in hydrogen storage allows investigation of the impact of inflexible hydrogen production on hydrogen and heat costs.

5
Results

Chapter 5 is organised as follows. Section 5.1 demonstrates how using waste heat from hydrogen production in Gothenburg's district heating system impacts the generation of and investments in heat generation technologies as well as the WHR system. Section 5.2 illustrates how the heat production cost, hydrogen production cost and total system cost differ between the scenarios investigated in this work. Section 5.3 presents the impacts of adding an electricity tax on power-to-heat technology, allowing investments in thermal energy storage capacity and restricting investments in hydrogen storage capacity on the model results.

5.1 Impacts of waste heat recovery from electrolysis on the energy system

This section presents the effects of introducing excess heat from electrolysis on total heat generation in the 2050 Gothenburg energy system. Table 5.1 shows total system cost, hydrogen cost and heat cost for cases with and without a waste heat recovery system, i.e., *without WHR* and *with WHR*. It can be seen that utilising heat from hydrogen production, as applied in the *with WHR* case, leads to total system cost (Equation 4.1) reduction of 0.8% in comparison to *without WHR* case. In the *with WHR* case, the average marginal cost of heat and average marginal cost of hydrogen (Equations 4.8 and 4.7) decrease by 2.3% and 2.6%, respectively compared to the *without WHR* case. From the results, it can be concluded that it is cost-efficient to invest in a waste heat recovery system to utilise heat from hydrogen production.

Table 5.1: Modelling results for total system cost, average marginal cost of heat and average marginal cost of hydrogen.

Cost	Without WHR	With WHR
C^{tot} $[MEUR]$	361.4	358.5
C^{heat}_{avg} $[EUR/MWh]$	12.9	12.6
$C^{H_2}_{avg}$ $[EUR/MWh]$	61.6	60

Figure 5.1 shows total heat generation in GWh in Gothenburg for the *without WHR* (a) and *with WHR* (b) cases. In both investigated cases, large-scale HP covers over 33% and waste heat 38% of the heat generated. When investments in WHR systems are allowed, as in the *with WHR* case, heat production by large-scale EBs reduces

by 4% and large-scale HP by 6% compared to the case *without WHR*. Biogas-fuelled HOB, biomass-fuelled HOB and individual residential HPs remain unchanged for the investigated cases.

Electrolyser and WHR configurations are invested in to utilise heat generated from hydrogen production in the *with WHR* case. Specifically, HX coupled with AEL90 covers 6% and HP coupled with AEL80 covers 1% of the annual heat generation for the case *with WHR*. These two configurations are characterised by their relatively high waste heat temperature, contributing to high hydrogen production efficiency as well as the possibility of low-cost HX and high efficiency HP. Additionally, the lower investment cost of the electrolyser of type AEL compared to PEM. The modelling results show that the AEL electrolyser with a high waste heat temperature (80–90°C) is one of the most efficient configurations for utilising heat from hydrogen production, leading to a reduction in heat generation from power-to-heat technologies such as large-scale electric boilers and heat pumps.

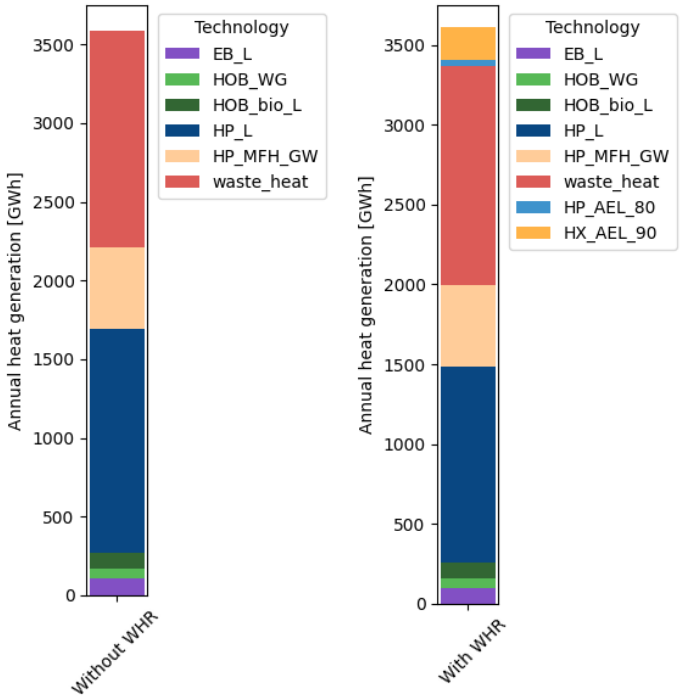

Figure 5.1: Total heat generation by technology and in Gothenburg *without WHR* (a) and *with WHR*(b). Heat generation technologies are large-scale EBs (EB_L), biomass-fuelled HOB (HOB_bio_L), biogas-fuelled HOB (HOB_WG_L), large-scale HP (HP_L), individual HP for multifamily housing (HP_MFH_GW), industrial waste heat (waste_heat), WHR HX connected to AEL90 (HX_AEL_90), WHR HP connected to AEL80 (HP_AEL_80) and PEM80 (HP_PEM_80).

5.1.1 Operation of heat generation technologies

Hydrogen demand is connected to the refineries in Rya, where electrolysers with potential for waste heat recovery are also installed. As a result, this region shows the largest change in heat generation between the investigated cases. To illustrate this difference, hourly heat generation in Rya was further analysed. Figure 5.2 shows hourly heat generation by respective technology in region Rya *without* (b) and *with WHR* (c), during hours 650-950 with large price variations of the imported electricity, with a maximum value of 660 EUR/MWh, and a minimum value of 25 EUR/MWh (a).

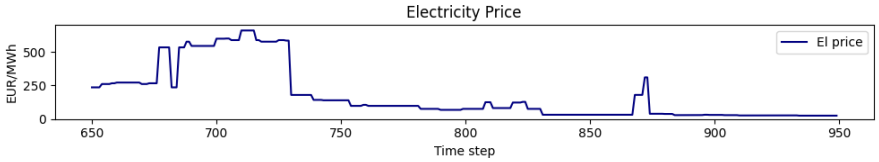

(a)

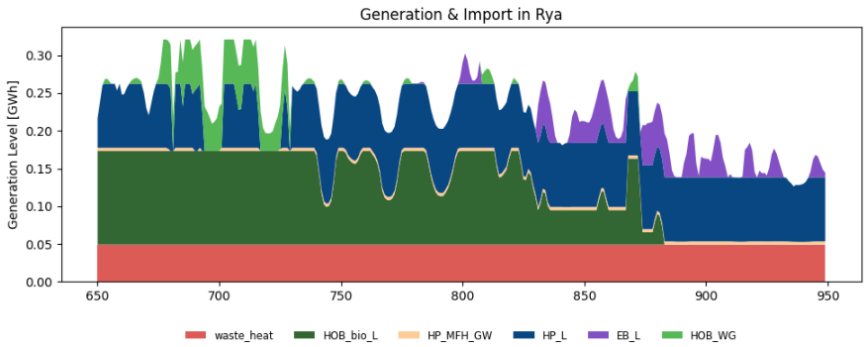

(b)

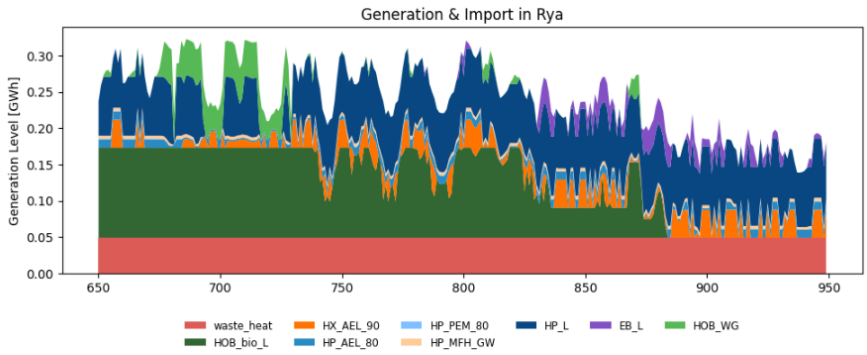

(c)

Figure 5.2: Electricity prices (a) and heat generation in region Rya *without WHR* (b) and *with WHR* (c), for hours 650-950. The electricity price varies between 25-660 EUR/MWh. Heat generation technologies are large-scale EBs (EB_L), biomass-fuelled HOB (HOB_bio_L), biogas-fuelled HOB (HOB_WG_L), large-scale HP (HP_L), individual HP for multifamily housing (HP_MFH_GW), industrial waste heat (waste_heat), WHR HX connected to AEL90 (HX_AEL_90), WHR HP connected to AEL80 (HP_AEL_80) and PEM80 (HP_PEM_80).

For both cases, biomass-fuelled HOBs have a higher generation during high electricity prices, and during peak prices, the biogas-fuelled HOB is operating as well. These HOBs are not invested in by the model, but were pre-existing. The individual multifamily housing HPs remain at a low level, and industrial waste heat is delivered at a constant level for both cases. When introducing WHR, as in the *with WHR* case, more variations are introduced in the generation profile. Large-scale EBs and HPs operate in a similar pattern, however, at a smaller capacity. These are the two technologies which is mainly replaced by electrolysis WHR. During the longest and highest electricity price peak, around hours 675–725, waste heat from the WHR heat exchanger (connected to AEL90) decreases as the electrolyser operates at minimum load due to high electricity costs. The WHR heat pump (connected to AEL80) produces even less heat, constrained by both the electrolyser's minimum load and the additional electricity cost of running the heat pump.

The introduction of waste heat recovery from electrolysis is primarily replacing large-scale electric boilers and heat pumps. Pre-existing biomass- and biogas-fuelled HOBs continue to play a key role during high electricity price periods, while WHR output is limited under these conditions due to reduced electrolyser operation and the cost of running associated heat pumps.

5.1.2 Operation of waste heat recovery systems

Table 5.2 shows investments in electrolysers and hydrogen storage for the *with WHR* and *without WHR* cases.

Table 5.2: Investments in electrolysers and hydrogen storage for *with WHR* and *without WHR* cases.

Electrolyser	without WHR	with WHR
AEL90 [MW]	296.4	239.8
AEL80 [MW]		58.6
Hydrogen storage [GWh]	16.1	14.6

In the *without WHR* case, hydrogen storage is used more extensively, both in larger capacity and with 4.5% more cycling over the year. The WHR paired electrolysers have additional value in running since they also produce heat, while the non-coupled electrolyser rather avoids operation during these hours and discharges the storage, to then charge it at a higher rate. It is expected that a larger hydrogen storage is related to a larger electrolyser capacity; however, the case *with WHR* has an 8.3% smaller storage and a 2% larger electrolyser capacity. This is linked to the lower efficiency of the AEL80 electrolyser, which is chosen as a second electrolyser in the *with WHR* case because of its advantageous heat characteristics; its availability (as the heat exchanger becomes unavailable when district heating supply temperatures exceed the limit set by Equation 2.1), and the high efficiency of the AEL80's connected heat pump. For the case *with WHR*, AEL90 produces 80% of the hydrogen demand, and AEL80 the remaining 20%.

Figure 5.3 shows hydrogen production during hours 7150-7250 of the year, with a price range of 12 to 115 EUR/MWh for imported electricity. The top panel shows AEL90 operation for the case *without WHR*, the second shows AEL90 operation for the case *with WHR*. Operation of AEL80 for the case *with WHR* is disregarded, since mainly the AEL90 satisfies the hydrogen demand. The third and fourth panel displays electricity price and heat demand.

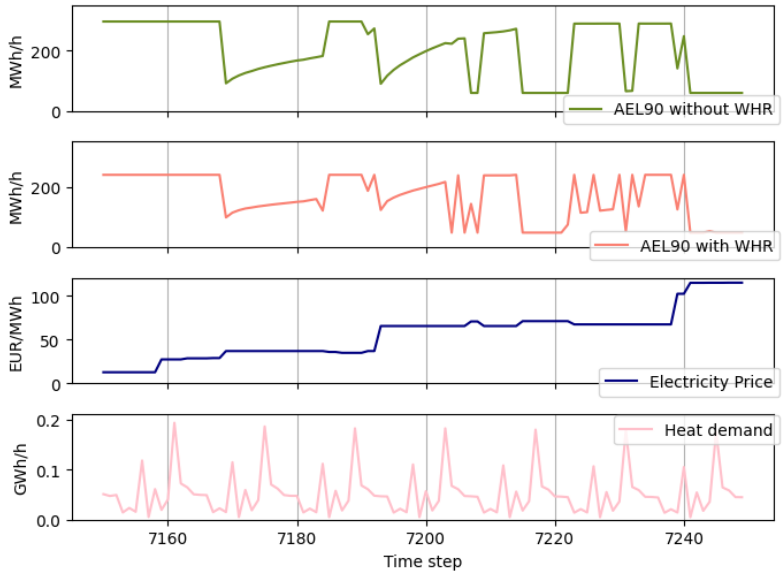

Figure 5.3: Hours 7150-7250, corresponding to the imported electricity price range of 12-115 EUR/MWh. The top panel shows electrolyser operation *without WHR*. The second show operation *with WHR*. The third panel displays electricity prices, and the fourth shows heat demand.

For both cases, the electrolyser is operating at maximum capacity continuously during low electricity prices, as seen from hours 7150 to 7170. When the electricity price exceeds 100 EUR/MWh, as seen around timestep 7240, electrolysers for both cases dip to minimum load. At mid-price levels (hours 7170–7240), operation differs between the cases. In the *with WHR* case, electrolyser output is driven by both electricity price and heat demand, sometimes increasing to supply heat and generate additional value, and sometimes decreasing when heat demand is low. This reflects the influence of sector coupling, in contrast to the *without WHR* case, where operation is primarily driven by electricity prices. Heat demand impacts hydrogen production when investments in WHR for electrolysis are allowed, as applied in *with WHR* scenario. The model has perfect foresight of the electricity prices, which impacts the operational strategy of electrolysers and sensitivity to electricity prices, such as AEL90 rapidly ramping up to full load for a slight price drop around timestep 7210, and reducing to minimum load in response to a minor price increase before timestep 7220.

Introducing WHR from electrolysers shifts hydrogen production from being solely a cost driven by electricity consumption to also generating revenue by supplying heat, and replacing large-scale HP and EB generation.

5.2 Impacts of waste heat recovery process configurations

Figure 5.4 shows the increase in average marginal cost of hydrogen in % (y-axis), in total system cost in % (colour gradient) and in average marginal cost of heat in % (x-axis). For the *no AEL90* case, investments in alkaline electrolyser with waste heat temperature of 90°C are not allowed. For the *no AEL90/80* case, the possibility to invest in alkaline electrolysers with waste heat temperatures of 80°C and 90°C was removed. In the *PEM* case, the possibility to invest in all AEL units was removed, and finally, in the *PEM50* case, the only electrolyser availible for investment in the model was a PEM electrolyser operating at 50°C. These cases are compared to the reference case *with WHR* with all WHR configurations available (See Section 2.3, Table 2.2).

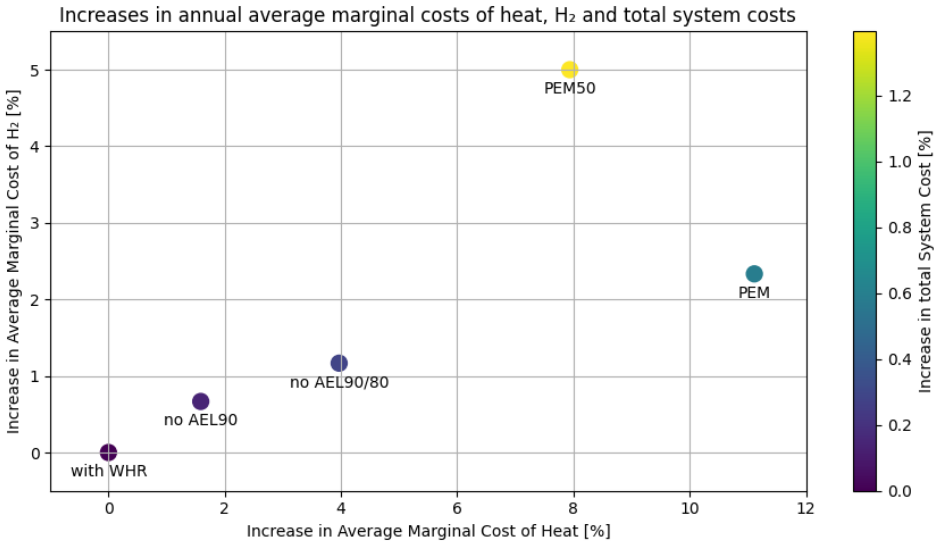

Figure 5.4: Increase in average marginal cost of hydrogen(H_2) in % (y-axis), in total system cost in (colour gradient) and in average marginal cost of heat in % (x-axis) for *no AEL90*, *no AEL90/80*, *PEM* and *PEM50* cases in comparison to the *with WHR* case.

As seen in the Figure 5.4, the differences in average marginal cost of hydrogen (ca. 0.7-5%), heat (ca. 1.8-11%) and total system costs(ca. 0-1.4%) are small between the cases. The *with WHR* case, which is able to invest in all eight WHR configurations studied, results in the lowest system costs and serves as the reference when comparing cost increases between the cases. From Figure 5.4, it can be seen that hydrogen and heat costs do not increase linearly between the cases. The *no AEL90* and *no AEL90/80* cases results in a 0.7% and 1.2% increase in the cost of hydrogen and a 1.6% and 4% increase in the cost of heat, respectively, compared to the *with WHR* case. This shows that, as higher efficiency and operating temperature AEL electrolysers are removed, both the cost of heat and hydrogen increase due to investments in electrolysers with lower operating temperatures. Conversely, for

the *PEM* and *PEM50* cases, this relationship is not observed. The *PEM50* case increases the cost of heat from the reference case to only 7.9%, whilst the *PEM* case, where all PEM electrolysers are available, the cost of heat increases to 11.1%. The cost of hydrogen increases as operating temperatures and efficiencies fall (2.3% for the *PEM* case and 5% for the *PEM50* case), which indicates that despite the total system costs increasing as higher efficiency and operating temperature PEM electrolysers are removed (0.6% for *PEM* and 1.4% for *PEM50*), the cost of heat is reduced with lower efficiency and operating temperature PEM electrolysers.

Figure 5.5 shows the annual heat generation in Gothenburg. The Figure illustrates when the electrolyser WHR is unavailable (a), and how heat generation shifts under different electrolyser availability constraints is detailed in (b). Additionally, Table 5.3, shows the invested electrolyser and WHR capacities for each case studied.

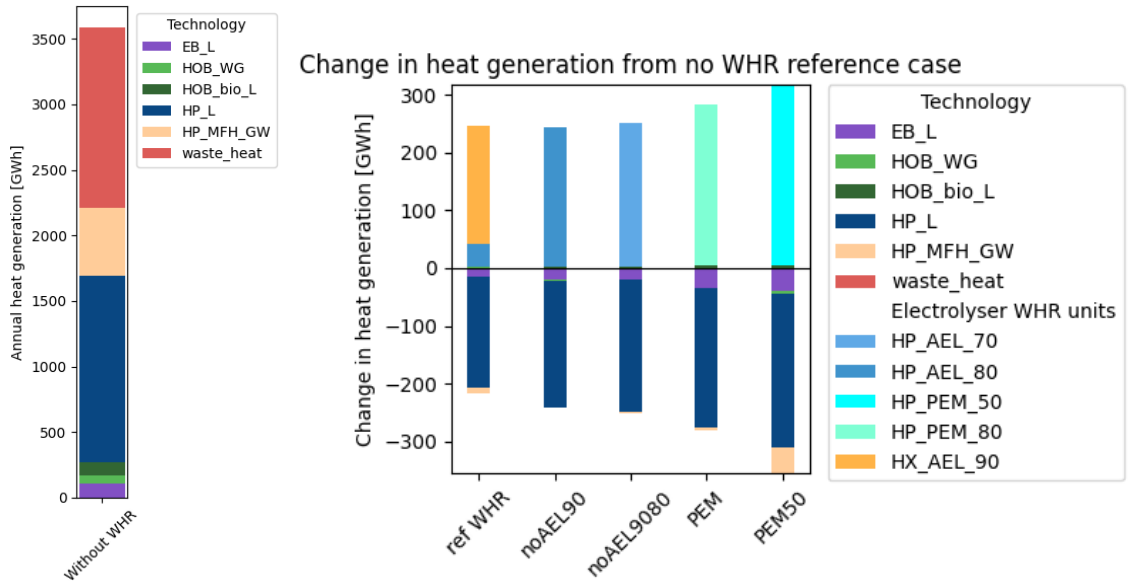

(a) **(b)**

Figure 5.5: Annual heat generation in GWh in Gothenburg for the Without WHR case (a) and the change in heat generation in GWh for with WHR, for the reference case *with WHR*, *no AEL90*, *no AEL9080*, *PEM* and *PEM50* cases in comparison to *without WHR* case (b). Positive values for the change in heat generation reflect an increase in generation, whereas negative values indicate a decrease. Heat generation technologies are large-scale EBs (EB_L), biomass-fuelled HOB (HOB_bio_L), biogas-fuelled HOB (HOB_WG_L), large-scale HP (HP_L), individual HP for multifamily housing (HP_MFH_GW), industrial waste heat (waste_heat), WHR HX connected to AEL90 (HX_AEL_90), WHR HP connected to AEL80 (HP_AEL_80), AEL70 (HP_AEL_70), PEM80 (HP_PEM_80) and PEM50 (HP_PEM_50).

Table 5.3: New electrolyser and WHR capacities for the cases studied

Case	Type	Technology	Capacity [MW]
Refererence with WHR	Electrolyser	AEL90	239.8
	WHR	HX AEL90	38.6
	Electrolyser	AEL80	58.6
	WHR	HP AEL80	1.4
No AEL90	Electrolyser	AEL80	285.5
	WHR	HP AEL80	6.8
No AEL90/80	Electrolyser	AEL70	286.2
	WHR	HP AEL70	7.3
PEM	Electrolyser	PEM80	390
	WHR	HP PEM80	11.3
PEM50	Electrolyser	PEM50	387
	WHR	HP PEM50	22.7

As seen in Figure 5.5b, all of the studied WHR cases mainly replace large-scale HP generation and, to a lesser extent, individual HP and EB generation when compared to the reference case *without WHR*. The reference case *with WHR* invested in both AEL90 with HX and AEL80 with HP, and was the most cost-effective version of the studied cases. This case utilises the most efficient electrolysers in terms of hydrogen production and as a result, the lowest producers of electrolyser waste heat at 242 GWh/y, which replaces 213 GWh/y of mainly large-scale HP generation.

The *no AEL90* case removed the model's ability to invest in HX, and thus, the generation of heat from WHR is only supplied with AEL80 with HP. As seen in the figure, even though the annual generation of WHR heat in the *no AEL90* case is the same as the annual generation of heat in the reference case *with WHR*, the no AEL90 case replaces more heat generation from other sources compared to the *without WHR* reference case. The *no AEL90* case replaces 12% more heat generation than the reference case *with WHR*, and this is due to the increase in flexibility that arises when utilising HP, which is always available, compared to HX. Furthermore, HP has a higher efficiency in heat generation than HX, and thus can produce more.

The Figure also shows the similarities in heat generation from WHR between the *no AEL90* and *no AEL90/80* cases. Table 5.3 shows that this is true with respect to installed capacity as well, with the AEL80 (285.5 GW) with accompanying HP (6.8 GW) and AEL70 (286.2 GW) with accompanying HP (7.3 GW) being extremely similar. The small increase in heat generation of 3% is caused by the electrolysers' small difference in waste heat efficiency of AEL70 compared to AEL80 of 0.7%.

The *PEM* case, where a PEM80 electrolyser is installed with a HP represents a large increase in both heat generation (278 GWh) from WHR and replaced generation (276 GWh). This increase is caused by the difference in efficiency and ability to utilise the hydrogen storage fully, thanks to the full load flexibility of PEM electrolysers. This can be seen from the installed capacities of both the PEM80 electrolyser of 390 MW and the HP of 11.3 MW. The large increase in capacity is caused by the PEM80 electrolyser being able to shut down fully as opposed to the AEL electrolysers, which can run at 20% load capacity at the lowest.

The PEM50 electrolyser in the *PEM50* case has similar, and even slightly lower, levels of installed capacity at 387 GW. However, it produces more heat annually (311 GWh) as seen in Figure 5.5b and even replaces some individual heat pumps in addition to the increased replacement of HP and EB units (349 GWh of total replaced technologies, of which 43 GWh is individual HPs). The lower efficiency indicates that even though the installed capacity did not change, it needs to operate for more hours of the year to deliver the same amount of hydrogen and thus the generation of waste heat increases.

5.2.1 Operational differences between AEL and PEM

Figure 5.6 shows how much available waste heat is produced for the no AEL90/80 case compared to the reference *with WHR* case.

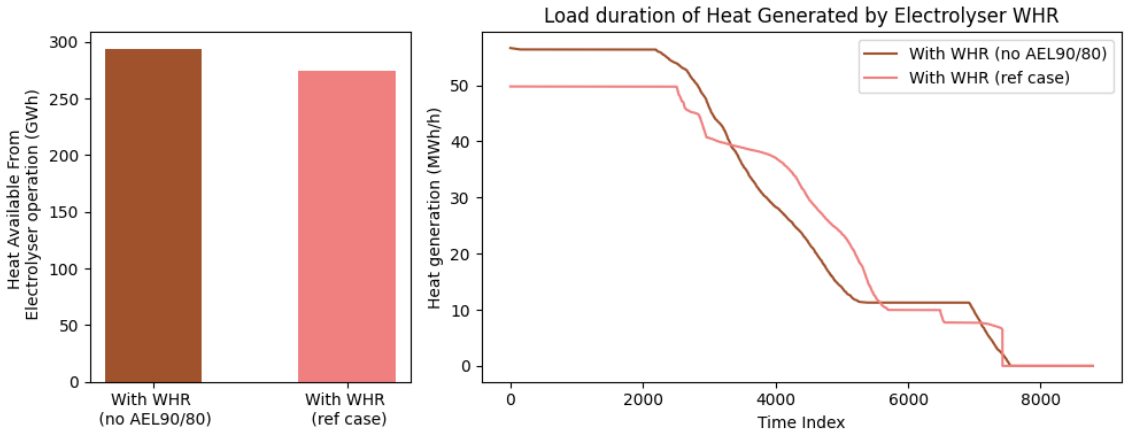

Figure 5.6: The left panel shows the available heat from electrolyser operation for the *no AEL90/80* case and for the reference case *with WHR*. The right panel displays the corresponding load duration curves for the accumulated heat generation from the WHR units for both cases.

The *no AEL90/80* case results in approximately 7% more available heat over the year compared to the reference case. As seen in the load duration curves, both scenarios supply heat for a similar number of hours and operate at full capacity for roughly the same duration. However, in the *no AEL90/80* case, operation occurs at higher levels during the full-capacity hours. This is due to improved efficiency during specific hours, partly driven by a higher COP for the heat pump when the waste heat and district heating supply temperatures are closer, allowing for more efficient use of the available capacity.

In comparison, Figure 5.7 shows available heat from the electrolyser as well as the load duration curve of the heat generated for the *PEM* case compared to the *with WHR* reference case. The figures clearly illustrate the ability of the PEM 80 electrolyser to change its operational load from 0-100% compared to the AEL electrolysers 20-100%. The model opts to oversize the electrolyser capacity of PEM80, leading to higher generation volumes of both hydrogen and heat from the WHR technology, but at fewer full load hours compared to *with WHR* reference case and the *no AEL90/80* case.

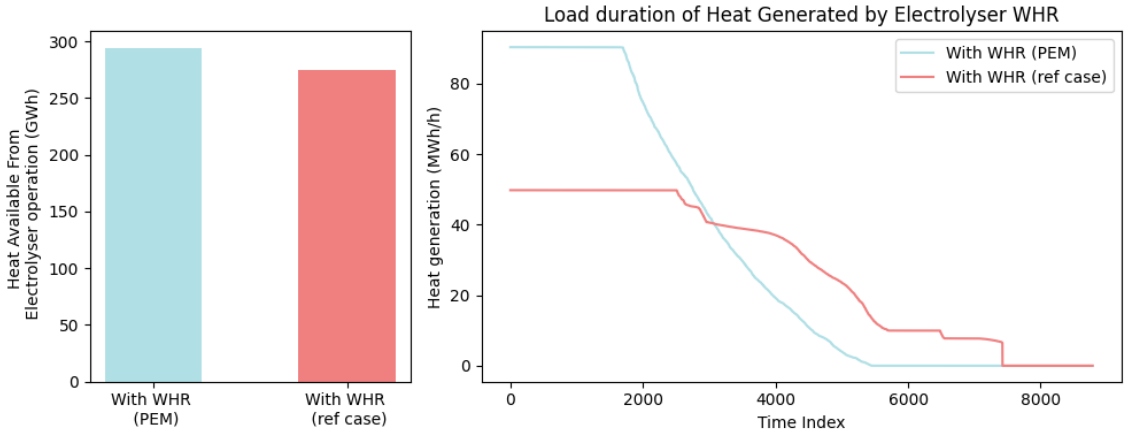

Figure 5.7: Available heat over a year (left) and load duration curve of heat generated by electrolyser WHR units (right) for the *PEM* case compared to the reference case *with WHR*.

Total available heat and how heat is generated by the WHR technologies are shown in Figure 5.8 for the *PEM50* case compared with the reference case *with WHR*. The total available heat of the low temperature PEM electrolyser is higher than the *with WHR* case due to the higher waste heat efficiency, which is directly linked to the larger heat losses in hydrogen production. The load flexibility enables the PEM electrolyser to go down to 0% of load, and thus the electrolyser requires a higher capacity to produce all necessary hydrogen when it is operating. These characteristics lead to either no electrolyser waste heat availability or a relatively large amount of heat availability, as clearly demonstrated in Figure 5.8 (right).

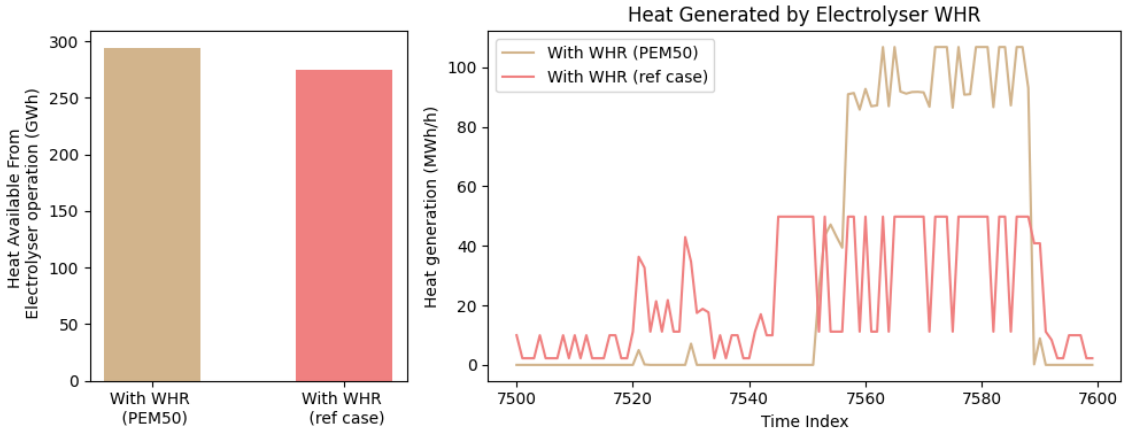

Figure 5.8: Available heat over a year (left) and heat generation during 100h by electrolyser WHR units (right) for the *PEM50* case compared to the reference case *with WHR*

5.3 Sensitivity analysis

The results from the sensitivity analysis are presented in this chapter. All scenarios studied in the sensitivity analysis are compared to the most cost-optimal solution from the results; the reference case *with WHR*. This is done with the aim of investigating how the changes to certain inputs of the model alter the previously presented results and to scrutinise them further. In the following subsections, three inputs used for the sensitivity analysis will be introduced, and their results will be presented.

5.3.1 Tax on Electricity-Consuming Heat Generation

This sensitivity analysis explores the system changes that occur when introducing taxation on PtH technologies. Table 5.4 shows the total system cost and average marginal cost for heat and hydrogen for two different electricity tax schemes, compared to the reference case *with WHR*. The two tax scenarios are: one where all power-to-heat (PtH) technologies are taxed, and another where only individual heat pumps (indHP) are taxed.

Table 5.4: Cost comparison across scenarios: reference case *with WHR*, tax on all PtH technologies, and tax on private PtH technologies (indHP)

Cost	WHR ref	tax PtH	tax indHP
C^{tot} [MEUR]	358.5	384.4	360.3
C^{heat}_{avg} [EUR/MWh]	12.6	20	13.8
$C^{H_2}_{avg}$ [EUR/MWh]	60	58.5	60

The scenario where all PtH technologies are taxed results in the highest system cost, increasing by 7.2% compared to the reference case *with WHR*. The average heat cost rises significantly, to €20/MWh, while the hydrogen cost remains comparable. This is caused by a larger share of the total heating demand being supplied by biomass HOB plants with accompanying fuel costs, and the still present, now more expensive, PtH technologies to a lesser extent. The tax on only indHP results in a total system cost increase of 0.5%, indicating a more cost-efficient approach to steering heat system design in favour of DH through targeted taxation. The small increase in cost is caused by the system opting to invest in centralised DH heating, without increased cost of taxation, instead of relying on individual heat pumps.

The changes in heat generation and technology utilisation are shown in Figure 5.9. The subfigures (a), (b) and (c) display the stacked heat load duration curves for each scenario. The reference case *with WHR* (Figure 5.9a) is dominated by electricity-based technologies, especially during mid- and low-load periods. When all PtH technologies are taxed (Figure 5.9b), their utilisation drops substantially, with combustion-based solutions increasing their shares instead. The tax on indHP (Figure 5.9c) causes a modest shift in generation but a drastic shift in source, preserving much of the original load structure while removing the contribution from individual HPs.

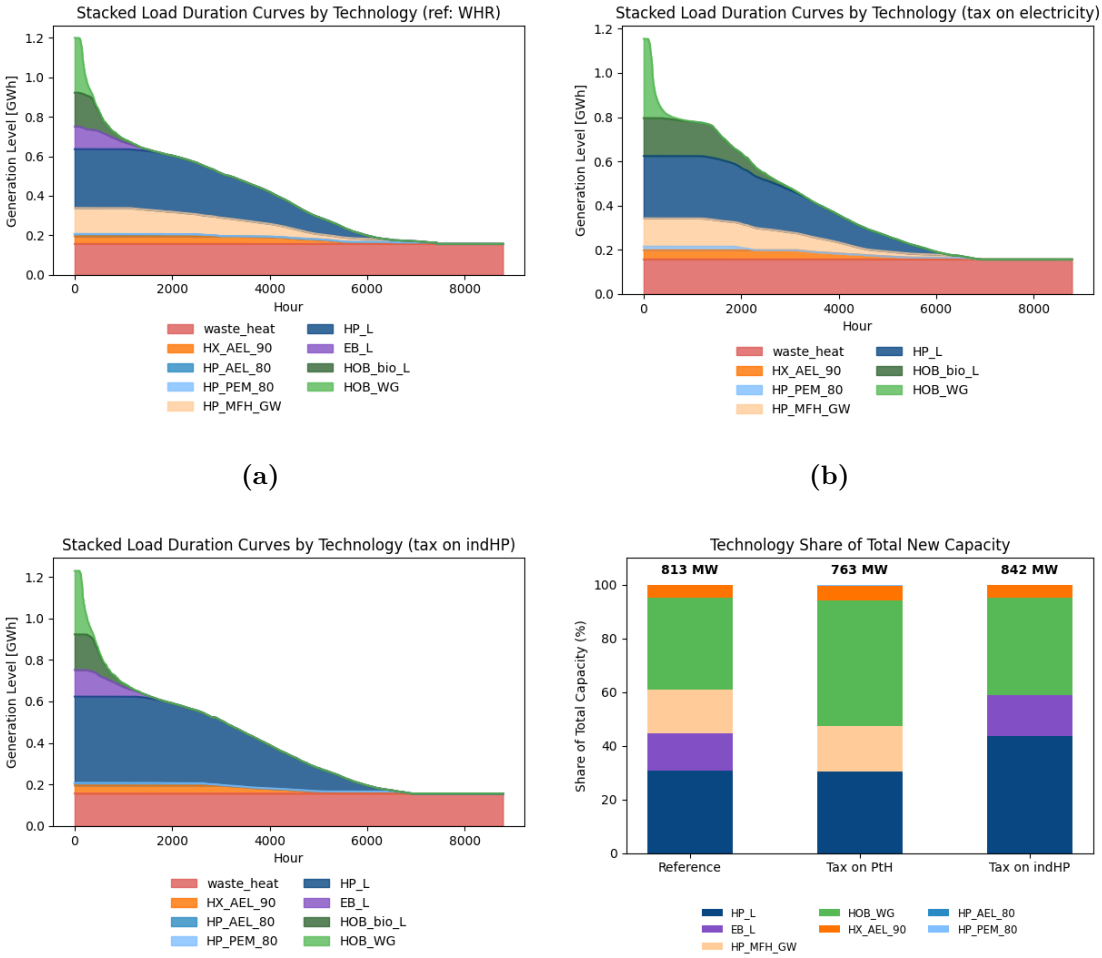

Figure 5.9: Comparison of heat load duration curves across different tax scenarios: (a) reference case *with WHR*, (b) tax on all PtH technologies, and (c) tax on private PtH technologies only. (d) shows the corresponding share of total new heat generation capacity by technology and scenario.

The tax scenarios clearly influence the system composition. As seen in Figure 5.9d, the total new installed capacity is lowest in the scenario with a full tax on all PtH technologies (763 MW), where a notable shift occurs toward increased reliance on thermal generation. In contrast, the tax on individual heat pumps leads to the highest total new capacity (842 MW). In this case, individual heat pumps are completely phased out and replaced by large-scale heat pumps, indicating a clear preference for district heating infrastructure. This transition happens with only a marginal increase in total system cost compared to the reference, suggesting that such a targeted tax would favour district heating companies by reinforcing centralised heat production without compromising economic efficiency to a large extent.

5.3.2 Investments in TES

This sensitivity analysis explores the system changes that occur when allowing the model to invest in tank TES in the Rya and East regions. This was done in order to investigate the resulting costs, generation and system composition change compared to the reference case *with WHR* when allowing current levels of installed capacity. Specifically, the capacities of 1 GWh storage were allowed in conjunction with the Renova WtE plant and in conjunction with the refineries in Rya, respectively. The result is that the model utilises the full allowed capacity, and invests in 1 GWh TES in East and Rya. The discharge of the two storages corresponds to 5% of Gothenburg's yearly heat demand, and the total system cost decreases by 0.5% compared to the reference case *with WHR*. Figure 5.10a, 5.10b and 5.10c show discharge of the two storages for three different import electricity price periods.

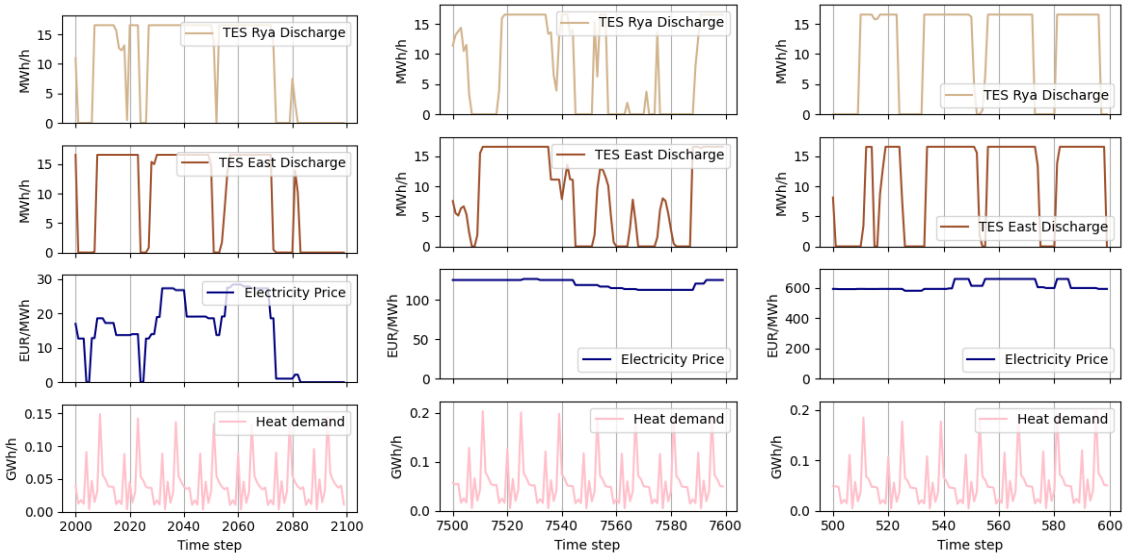

Figure 5.10: Discharge from TES in East and in Rya. The Figure presents three time periods selected based on differing electricity spot price ranges; (a) 0-28 EUR/MWh$_{el}$, (b) 112-126 EUR/MWh$_{el}$ and, (c) 580-660 EUR/MWh$_{el}$

The TES discharge patterns in the two regions are similar, generally increasing when electricity prices rise and decreasing when prices fall. The most notable change in thermal generation compared to the reference case *with WHR* is a 10 GWh reduction in large-scale EBs and a 6 GWh increase in large-scale HPs. The introduction of TES also reduces heat overproduction by 3.5%. Combined with the higher PtH efficiency of large-scale HPs compared to EBs, this leads to a 3% reduction in electricity use in Gothenburg, lowering the overall system cost.

5.3.3 No Investments in Hydrogen Storage

In this scenario, the ability of the model to invest in storage capacity for hydrogen is completely removed. This was done in order to investigate a scenario where the possibility of constructing LRC storage is found to be infeasible in the Västra Götaland region. Without storage, hydrogen must be produced and consumed simultaneously, reducing operational flexibility and potentially affecting both hydrogen and heat generation from WHR systems. Table 5.5 compares the total system cost and average marginal costs for heat and hydrogen between the reference case and the no-hydrogen storage scenario. While the total system cost increases slightly by 1%, the cost of heat actually decreases marginally. The average cost of hydrogen, however, increases by 2%.

Table 5.5: Cost comparison between the reference case with WHR and the scenario without access to hydrogen storage

Cost	WHR ref	no H_2 storage
C^{tot} [MEUR]	358.5	362.1
C^{heat}_{avg} [EUR/MWh]	12.6	12.5
$C^{H_2}_{avg}$ [EUR/MWh]	60	61.2

Figure 5.11 illustrates the changes in heat generation profiles and dispatch during a high electricity price event (with a peak of 660 [EUR/MWh]). As shown in the heat load duration curve (Figure 5.11b), the system without hydrogen storage leads to increased use of combustion-based technologies during peak-load events, compared to the reference case (Figure 5.11a). This shift is due to the reduced ability of electrolysers to operate flexibly and provide waste heat on demand. To further demonstrate this, Figures 5.11c and 5.11d show the dispatch of heat by source to meet the heating demand of the Sörred region, which imports heat from the Rya region where the WHR system is located. In both cases, biogas boilers are used to meet demand. However, a key difference lies in the operation of these generation technologies. With access to hydrogen storage, the system achieves a smoother production curve, resulting in lower investment in peaking capacity (13 MW versus 26 MW of biogas boiler capacity in Sörred). The dispatch of heat across all heat regions during this event is provided in Appendix A.3.1.

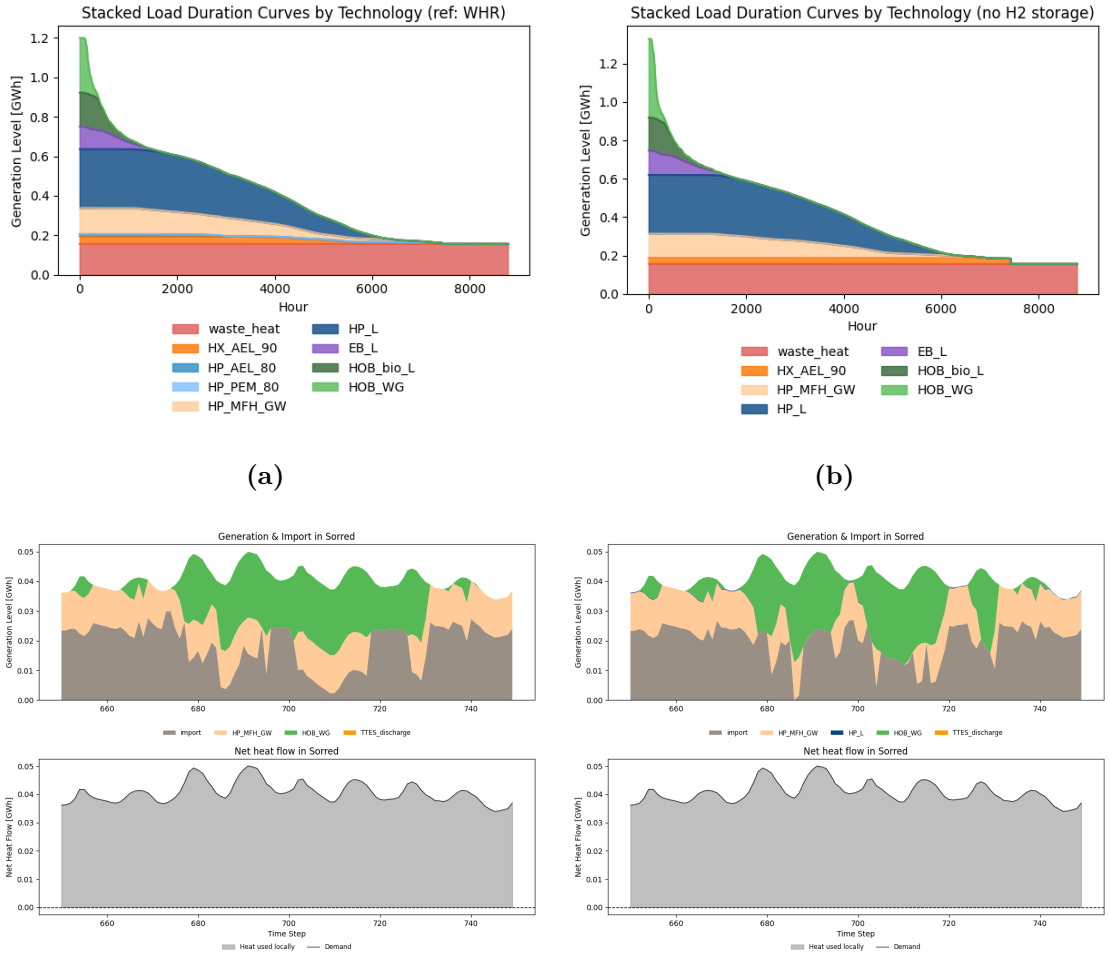

Figure 5.11: Comparison of heat load duration curves (with- and without access to hydrogen storage) scenarios: (a) reference case with WHR, (b) and no hydrogen storage. (c) and (d) shows the generation of heat in the Sörred region during a high electricity price event (peak of 660 [EUR/MWh]) with and without access to hydrogen storage, respectively.

Figure 5.12 shows installed electrolyser capacity as well as WHR load duration over one year, comparing a system with hydrogen storage and without. The electrolyser capacity is 34% smaller when no storage is available and the electrolyser operates continuously. This means that waste heat from the electrolyser is always available, and it is used at max capacity for most hours of the year. This shows that even though the heat is delivered to the DH system more predictably from WHR, the system has lost a flexibility measure that acted to dampen variations in generation.

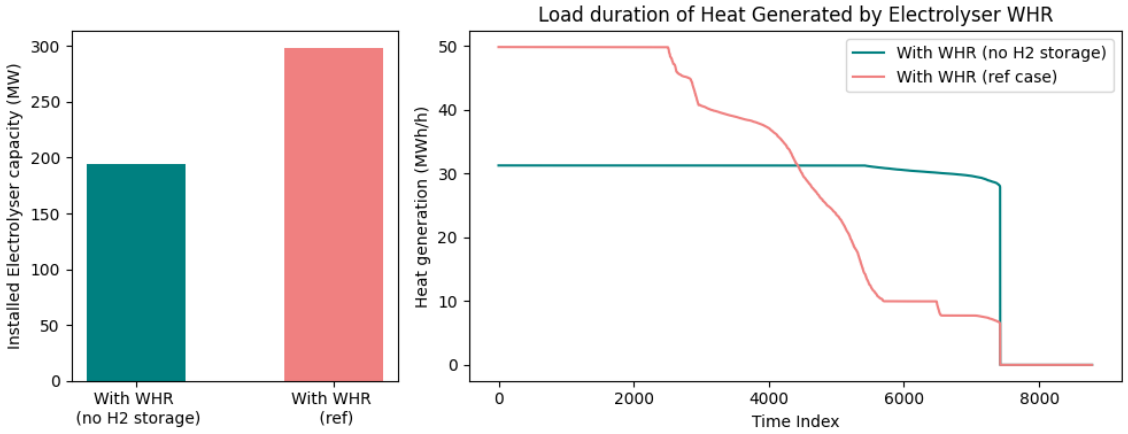

Figure 5.12: Installed electrolyser capacity (left) and load duration of associated WHR units for reference case compared to case without hydrogen storage.

6
Discussion

The implications of integrating waste heat from electrolysers into Gothenburg's existing district heating network were investigated in this study. The main findings from the modelling show that including WHR from hydrogen production can reduce total system cost by 1%, corresponding to 3 MEUR, in comparison to the case *without WHR* and replace ca. 200 GWh of industrial HP heat generation. All electrolyser types can supply a similar amount of waste heat, but differences in load flexibility affect their hourly availability. PEM electrolysers offer high load flexibility, which results in a higher cost of heat. They are also more investment-intensive than AEL electrolysers, contributing to a higher total system cost. However, their dynamic properties make them well-suited for flexible electricity consumption, as seen from their operational patterns of high peak production at lower occurrences compared to AEL.

While the model provides valuable insights into the cost-optimal configurations of electrolysers and WHR technologies, it operates under assumptions that must be discussed. Since the system dispatch of heat, electricity, and hydrogen has perfect foresight of electricity prices and future demands, the model's operational patterns may not fully reflect real-world behaviour, where limited predictability typically leads to more cautious and less extreme dispatch strategies. Rapid changes, such as electrolysers shifting from minimum to maximum load in response to small electricity price signals, may therefore be overestimated, potentially overstating the cost savings from electricity price-driven operation. While price forecasts and the ability of electrolysers to shift production load are reliable, the perfect foresight in the model provides an operational advantage that doesn't exist in reality.

Additionally, several key parameters in the model were based on estimated variations in district heating supply temperatures to maintain linearity. For example, the coefficient of performance (COP) of heat pumps was set according to an assumed temperature profile rather than modelled dynamically. This means the model does not capture the full dynamics when integrating WHR, especially during periods with significant fluctuations in supply temperature.

The current AEL constraint, which describes the minimum production (see Table 4.3), captures only the lower flexibility bounds. The constraint formulation can lead to undervaluing AEL's ability to shut down and restart. Moreover, the absence of degradation costs, thermal inertia in electrolyser and WHR operation, and start-up costs could conceal long-term performance challenges and investment risks.

6.1 Electrolyser configuration's impact on WHR potential

The WHR system configurations comparisons indicate that a higher waste heat temperature provides lower hydrogen and heat production costs in comparison to a lower waste heat temperature. Utilising HX for WHR was found to be the most cost-effective solution when available, primarily due to its low investment costs and lack of running costs. While HPs are more capital-intensive and their operation depends on electricity prices, access to high-temperature waste heat improves their COP due to the lower required temperature lift.

The potential of integrating electrolyser WHR into a fourth-generation district heating (4GDH) system, characterised by supply temperatures below 70°C, needs to be investigated further. For this type of system, HX could be integrated with a larger share of electrolyser units.

Assuming current investment cost trajectories for PEM and AEL technologies by 2050, AEL is associated with lower total system and hydrogen production costs compared to PEM electrolysers. The value of PEM's dynamic load flexibility depends on the ownership structure of the electrolyser. However, the modelled flexibility of AEL is subject to certain limitations. Specifically, AEL can operate only within a load range of 20–100%, but it can be shut down and restarted with a start-up time of approximately 1–2 hours. Further investigation into the effects of integrating both the ability of AEL to shut down and its accompanying start-up time would be interesting for future research.

6.2 Actor Perspective in System-Based Energy Planning

The aim of this thesis was to identify the most cost-effective composition of the Gothenburg energy system in 2050 when integrating electrolyser WHR. To achieve this, the system is viewed on a macro-level, without consideration for the ownership structure of individual technologies.

While the results are cost-optimal on a societal level, conflicts may arise when considering the interests of specific actors within the system. A potential central point of conflict could lie in the operation of the WHR system, which bridges hydrogen production (typically owned by an industrial actor) and the DH system (operated by a DH company). The results indicate an inverse correlation between periods of optimal hydrogen production (driven by electricity prices and hydrogen demand) and periods of peak heat demand. This temporal mismatch reduces the reliability of heat supply from electrolyser WHR, from the perspective of a DH company. As a result, the DH company would benefit from operational agreements that ensure that the electrolyser, and therefore the WHR unit, runs during periods of high heat

demand. If such agreements are not in place, there is a risk that the WHR unit may be unavailable when most needed, reducing the technology's value in supporting the heat system. However, this mismatch can be addressed by introducing incentives for flexible heat generation that is responsive to heat demand. Variable heat pricing could support a more flexible heat market and increase the value of operating electrolysis units coupled with waste heat recovery during periods of high heat demand. Additional thermal energy storage would allow heat produced during periods of low demand to be stored and used when heating needs are higher. Storage solutions can improve the utilisation of surplus renewable electricity, such as from solar and wind, for hydrogen production, thereby contributing to grid balancing.

Additionally, the sensitivity analysis involving taxation on PtH technologies (Section 5.3.1) highlights important policy-related implications for DH companies. The introduction of a flat tax on PtH sources in the model resulted in increased investments in thermal peaking technologies and maintained levels of privately owned individual heat pumps. While the system is cost-optimal from a societal point of view under these conditions, this outcome, as well as the reference case with WHR that also has a large share of heat generation from individual HP, introduces operational uncertainty for DH operators. If households can switch heating sources on demand, the resulting fluctuations in DH heat demand complicate operational planning and would lead to potential revenue losses for the DH company. This instability may undermine the economic sustainability of centralised DH systems. The results also suggest that removing taxes from PtH units owned by the DH company eliminates this issue, preserving centralised coordination. However, this raises the question: should policymakers intervene to support the economic stability of DH companies at the expense of consumer choice and potential cost savings? While centralised heat production offers potential benefits in terms of efficiency and emissions reduction, as outlined in Chapter 3, further research is needed to explore appropriate and equitable policy interventions.

Coordination mechanisms will be key to aligning actor incentives and preserving the benefits of a stable, centralised district heating system in a transitioning energy system.

7
Conclusion

This thesis aimed to assess the techno-economic implications of integrating waste heat recovery (WHR) from electrolysers into the district heating system of Gothenburg. A linear optimisation model was applied to find the cost-optimal energy system composition from a societal perspective in the year 2050.

The modelling results show that heat recovery from hydrogen production reduces the total system cost of Gothenburg by 1%, corresponding to 3 MEUR, in comparison to the case when heat from hydrogen production is not utilised. This indicates that the integration of heat recovery from electrolysers is beneficial from a system perspective and has an even greater potential for cost reductions with higher hydrogen demand. In addition, it was found that the average cost of hydrogen production and average cost of heat production can be reduced up to 2.3% and 3.5%, respectively, for the case when investments in the WHR system are allowed, *with WHR*, in comparison to the case *without WHR*. The integration of the WHR system leads to a reduction of PtH technologies (large-scale EB and HP). This confirms the value of leveraging excess heat from hydrogen production to support the DH network.

Electrolysers with high waste heat temperature, such as Alkaline electrolyser (AEL) operating at 90°C, result in the lowest total system cost compared to other electrolyser and WHR configurations (see Figure 5.4). For the cases when investments only in PEM electrolysers are allowed, such as *PEM* and *PEM50*, the total system cost increases by 4.7% and 5.5% compared to the lowest total system cost case with AEL operating at a temperature of 90°C *with WHR*. The higher system cost is primarily driven by the larger investment cost of PEM electrolysers, rather than the cost of electrolysis WHR associated with this technology.

When investments in hydrogen storage are not allowed, the model results show that the cost of heat decreases by 1% and the cost of hydrogen increases by 2%, in comparison to the *with WHR* case. Introduction of TES storage results in a 0.5% reduction in total cost in comparison to the *with WHR* case. The modelling results describe a need for cooperation between hydrogen production and heat generation systems, which can lead to cost reduction of both hydrogen and heat as well as an increase in energy utilisation of electrolysers.

Bibliography

[1] European Commission, *Eu emissions trading system (eu ets)*, 2025. [Online]. Available: https://climate.ec.europa.eu/eu-action/eu-emissions-trading-system-eu-ets_en.

[2] European Commission, *European climate law*, 2021. [Online]. Available: https://climate.ec.europa.eu/eu-action/european-climate-law_en.

[3] STOA | Panel for the Future of Science and Technology, "The potential of hydrogen for decarbonising steel production," European Parliment, Tech. Rep., 2020. [Online]. Available: https://www.europarl.europa.eu/RegData/etudes/BRIE/2020/641552/EPRS_BRI(2020)641552_EN.pdf.

[4] Directorate-General for Defence Industry and space, European Commission, *The alliance for zero-emission aviation launches its vision towards electric and hydrogen flight in europe*, 2024. [Online]. Available: https://defence-industry-space.ec.europa.eu/alliance-zero-emission-aviation-launches-its-vision-towards-electric-and-hydrogen-flight-europe-2024-06-06_en.

[5] Directorate-General for Energy, *Hydrogen*, 2025. [Online]. Available: https://energy.ec.europa.eu/topics/eus-energy-system/hydrogen_en.

[6] Danish Energy Agency, *Technology data – renewable fuels*, Online, version 0012, First published in 2017, current version licensed under Attribution 4.0 International. Accessed: 2025-02-06, Carsten Niebuhrs Gade 43, 1577 Copenhagen, Denmark: Danish Energy Agency, 2024. [Online]. Available: https://ens.dk/en/analyses-and-statistics/technology-data-renewable-fuels.

[7] E. Rydegran, *Fjärrvärme*, Publicerat av Energiföretagen Sverige, 2025. [Online]. Available: https://www.energiforetagen.se/energifakta/fjarrvarme/.

[8] H. Böhm, S. Moser, S. Puschnigg, and A. Zauner, "Power-to-hydrogen district heating: Technology-based and infrastructure-oriented analysis of (future) sector coupling potentials," *International Journal of Hydrogen Energy*, vol. 46, no. 63, pp. 31 938–31 951, 2021, ISSN: 0360-3199. DOI: https://doi.org/10.1016/j.ijhydene.2021.06.233. [Online]. Available: https://www.sciencedirect.com/science/article/pii/S0360319921025477.

[9] E. H. Observatory, *Electrolyser cost*, 2024. [Online]. Available: https://observatory.clean-hydrogen.europa.eu/hydrogen-landscape/production-trade-and-cost/electrolyser-cost.

[10] IEA, "Global hydrogen review 2024," International Energy Agency, Report, 2024. [Online]. Available: https://iea.blob.core.windows.net/assets/89c1e382-dc59-46ca-aa47-9f7d41531ab5/GlobalHydrogenReview2024.pdf.

[11] A. Trattner, M. Hoeglinger, M.-G. Macherhammer, and M. Sartory, "Renewable hydrogen: Modular concepts from production over storage to the consumer," *Chemie Ingenieur Technik*, vol. 93, Feb. 2021. DOI: 10.1002/cite.202000197.

[12] M. Klingenhof *et al.*, "High-performance anion-exchange membrane water electrolysers using nix (x = fe,co,mn) catalyst-coated membranes with redox-active ni–o ligands," *Nature Catalysis*, vol. 7, pp. 1213–1222, Oct. 2024, Published: 28 October 2024. DOI: 10.1038/s41929-024-01238-w. [Online]. Available: https://www.nature.com/articles/s41929-024-01238-w.

[13] Y. Zuo *et al.*, "High-performance alkaline water electrolyzers based on ru-perturbed cu nanoplatelets cathode," *Nature Communications*, vol. 14, no. 1, p. 4680, 2023, Open access, published 04 August 2023. DOI: 10.1038/s41467-023-40320-z. [Online]. Available: https://www.nature.com/articles/s41467-023-40320-z.

[14] X. Sun, M. Chen, Y. Liu, and P. Vang Hendriksen, "Life time performance characterization of solid oxide electrolysis cells for hydrogen production," *ECS Transactions*, vol. 68, pp. 3359–3368, Jul. 2015. DOI: 10.1149/06801.3359ecst.

[15] A. Meriläinen, A. Kosonen, J. Jokisalo, R. Kosonen, P. Kauranen, and J. Ahola, "Techno-economic evaluation of waste heat recovery from an off-grid alkaline water electrolyzer plant and its application in a district heating network in finland," *Energy*, vol. 306, p. 132 181, 2024, ISSN: 0360-5442. DOI: https://doi.org/10.1016/j.energy.2024.132181. [Online]. Available: https://www.sciencedirect.com/science/article/pii/S0360544224019558.

[16] E. van der Roest, R. Bol, T. Fens, and A. van Wijk, "Utilisation of waste heat from pem electrolysers – unlocking local optimisation," *International Journal of Hydrogen Energy*, vol. 48, no. 72, pp. 27 872–27 891, 2023, ISSN: 0360-3199. DOI: https://doi.org/10.1016/j.ijhydene.2023.03.374. [Online]. Available: https://www.sciencedirect.com/science/article/pii/S0360319923015410.

[17] X. Jin *et al.*, "Feasibility investigation of thermal management and heat recovery of low-temperature hydrogen electrolysis systems," in *2024 IEEE PES Innovative Smart Grid Technologies Europe (ISGT EUROPE)*, Accessed: 2025-05-08, IEEE, 2024, pp. 1–5. DOI: 10.1109/ISGTEUROPE62998.2024.10863023. [Online]. Available: https://research.ebsco.com/linkprocessor/plink?id=c03ff5ae-e96a-341f-86d1-6656ab0544a4.

[18] N. Frassl, N. R. Sistani, Y. Wimmer, J. Kapeller, K. Maggauer, and J. Kathan, "Techno-ökonomische analyse der abwärmenutzung in der grünen wasserstoffproduktion: Eine simulationsstudie," German, *e & i Elektrotechnik und Informationstechnik*, vol. 141, no. 5, pp. 288–298, 2024, Accessed: 2025-05-08, ISSN: 0932-383X. DOI: 10.1007/s00502-024-01231-y. [Online]. Available: https://link.springer.com/article/10.1007/s00502-024-01231-y.

[19] A. Buttler and H. Spliethoff, "Current status of water electrolysis for energy storage, grid balancing and sector coupling via power-to-gas and power-to-liquids: A review," *Renewable and Sustainable Energy Reviews*, vol. 82, pp. 2440–2454, 2018, ISSN: 1364-0321. DOI: https://doi.org/10.1016/j.

rser.2017.09.003. [Online]. Available: https://www.sciencedirect.com/science/article/pii/S136403211731242X.

[20] S. Werner, "International review of district heating and cooling," *Energy*, vol. 137, pp. 617–631, 2017, ISSN: 0360-5442. DOI: https://doi.org/10.1016/j.energy.2017.04.045. [Online]. Available: https://www.sciencedirect.com/science/article/pii/S036054421730614X.

[21] J. Pelda, F. Stelter, and S. Holler, "Potential of integrating industrial waste heat and solar thermal energy into district heating networks in germany," *Energy*, vol. 203, p. 117 812, 2020, ISSN: 0360-5442. DOI: https://doi.org/10.1016/j.energy.2020.117812. [Online]. Available: https://www.sciencedirect.com/science/article/pii/S0360544220309191.

[22] J. Granath, *Göteborgs stads energiplan 2022–2030*, version 3, Fastställd av Kommunfullmäktige, Gällande från 2023-02-22, Dnr 0044/22, 2023. [Online]. Available: https://www4.goteborg.se/prod/Stadsledningskontoret/LIS/Verksamhetshandbok/Forfattn.nsf//30944AE15043B0DDC1258845003CE158/$File/C12574360024D6C7WEBVCPA387.pdf?OpenElement.

[23] Renova AB, *Här blir avfall till el och värme*, Accessed: 2025-03-24, 2024. [Online]. Available: https://www.renova.se/om-oss/anlaggningar/savenas-avfallskraftvarmeverk/.

[24] Renova AB, *Här blir avfall till el och värme: Avfallskraftvärmeverket i sävenäs, göteborg*, Broschyr, Renovas avfallskraftvärmeverk i Sävenäs är ett av världens mest effektiva anläggningar. Här hanteras upp till 550 000 ton avfall per år och producerar el och värme för samhällets behov., 2023. [Online]. Available: https://www.renova.se/globalassets/11.-pdf-er/har-blir-avfall-till-el-och-varme/har_blir_avfall_till_el_och_varme_2023.pdf.

[25] Naturvårdsverket, *Plastavfall*, Swedish Environmental Protection Agency, Accessed: 2025-01-10, 2025. [Online]. Available: https://www.naturvardsverket.se/amnesomraden/avfall/avfallslag/plastavfall/.

[26] R. van der Meer, E. D. Coninck, J. Helseth, K. Whiriskey, A. Perimenis, and A. Heberle, *A method to calculate the positive effects of ccs and ccu on climate change*, European Union's Horizon 2020 Research and Innovation Programme, Grant Agreement No 826051, Prepared on behalf of the Advisory Council of the European Zero Emission Technology and Innovation Platform (ETIP ZEP)., Jul. 2020. [Online]. Available: https://zeroemissionsplatform.eu/wp-content/uploads/A-method-to-calculate-the-positive-effects-of-CCS-and-CCU-on-climate-change-July-2020.pdf.

[27] J. Berg, "Feedstock recycling i ett plastreturraffinaderi: Teknoekonomi, hållbarhet och policy," RISE Research Institutes of Sweden AB, Tech. Rep. 47565-1, Nov. 2019, Final report for project 47565-1, covering the period 2019-03-01 to 2019-10-31. [Online]. Available: https://www.ri.se.

[28] Naturvårdsverket, *Hållbar plastanvändning*, Swedish Environmental Protection Agency, Accessed: 2024-08-22, 2024. [Online]. Available: https://www.naturvardsverket.se/amnesomraden/plast/hallbar-plastanvandning/.

[29] Renova AB, *Hållbarhetsredovisning 2024*, Online, Accessed: 2025-03-27, Box 156, 401 22 Göteborg: Renova AB, 2024. [Online]. Available: https://www.

renova.se/globalassets/11.-pdf-er/hallbarhetsredovisnigen/2024_renova_haellbarhetsredovisning_digital.pdf.

[30] A. Nurdiawati and F. Urban, "Towards deep decarbonisation of energy-intensive industries: A review of current status, technologies and policies," *Energies*, vol. 14, no. 9, 2021, ISSN: 1996-1073. [Online]. Available: https://www.mdpi.com/1996-1073/14/9/2408.

[31] Preem, "Sustainability report 2024," Preem AB, Tech. Rep., 2024. [Online]. Available: https://cms.preem.com/Content/documents/rapporter/hallbarhetsredovisningar/2024/preem_sustainability_report_2024.pdf.

[32] M. Edvall, L. Eriksson, S. Harvey, J. Kjärstad, and J. Larfeldt, "Vätgas på västkusten," RISE, RISE rapport 2022:31, Feb. 2022, Accessed: 2025-02-26. [Online]. Available: https://www.diva-portal.org/smash/get/diva2:1640678/FULLTEXT01.pdf.

[33] Å. Eliassion and E. Fahrman, "Utilization of industrial excess heat for co2 capture," Master's Thesis, Chalmers University of Technology, Gothenburg, Sweden, 2020. [Online]. Available: https://odr.chalmers.se/server/api/core/bitstreams/028f314d-bc3a-4a54-ab13-2beb813e9a7e/content.

[34] Directorate-General for Energy, *Renewable hydrogen*, 2025. [Online]. Available: https://energy.ec.europa.eu/topics/eus-energy-system/hydrogen/renewable-hydrogen_en.

[35] St1, "Game changer 2024, st1 nordic oy integrated report," st1, Tech. Rep., 2024. [Online]. Available: https://media.ffycdn.net/eu/st1/kyTJEvDYN9xf8PnTjSwQ.pdf?content_type=game_changer_report.

[36] S. Rosén, L. Göransson, M. Taljegård, and M. Lehtveer, "Modeling of a "hydrogen valley" to investigate the impact of a regional pipeline for hydrogen supply," *Frontiers in Energy Research*, vol. 12, no. 1420224, Aug. 2024, Accessed: 2025-02-26. DOI: 10.3389/fenrg.2024.1420224. [Online]. Available: https://research.chalmers.se/publication/542142/file/542142_Fulltext.pdf.

[37] Göteborg Energi, *Kapacitetsutmaningen*, Accessed: 2024-05-12, 2025. [Online]. Available: https://www.goteborgenergi.se/om-oss/vad-vi-gor/hallbarhet/kapacitetsutmaningen.

[38] S. I. Ngo, D. D. Nguyen, Y.-i. Lim, W. Kim, D. Seo, and W.-L. Yoon, "Computational fluid dynamics model on a compact-type steam methane reformer for highly-efficient hydrogen production from natural gas," in *13th International Symposium on Process Systems Engineering (PSE 2018)*, ser. Computer Aided Chemical Engineering, M. R. Eden, M. G. Ierapetritou, and G. P. Towler, Eds., vol. 44, Elsevier, 2018, pp. 307–312. DOI: https://doi.org/10.1016/B978-0-444-64241-7.50046-X. [Online]. Available: https://www.sciencedirect.com/science/article/pii/B978044464241750046X.

[39] V. Heinisch, L. Göransson, M. Odenberger, and F. Johnsson, "Interconnection of the electricity and heating sectors to support the energy transition in cities," *International Journal of Sustainable Energy Planning and Management*, vol. 24, Oct. 2019. DOI: 10.5278/ijsepm.3328. [Online]. Available: https://journals.aau.dk/index.php/sepm/article/view/3328.

[40] J. Bertilsson, L. Göransson, and F. Johnsson, "Impact of energy-related properties of cities on optimal urban energy system design," *Energies*, vol. 17, no. 15, 2024, ISSN: 1996-1073. DOI: 10.3390/en17153813. [Online]. Available: https://www.mdpi.com/1996-1073/17/15/3813.

[41] H. Yu, L. Göransson, and F. Johnsson, "Modeling of future district heating: Waste heat and network refurbishment dynamics," *manuscript*, 2025.

[42] P. Håkansson and L. Johansson, "Thermal storage valuation in gothenburg district heating system," Master's Thesis, Chalmers University of Technology, Gothenburg, Sweden, 2023. [Online]. Available: https://odr.chalmers.se/items/cfc7e575-91fe-4d62-9a0f-13b605a161cf.

[43] Göteborg Energi, *Därför byggde vi göteborgs största termos*, Accessed: 2025-05-16, Göteborg Energi, 2018. [Online]. Available: https://www.goteborgenergi.se/i-var-stad/artikelbank/darfor-byggde-vi-goteborgs-storsta-termos.

[44] L. Göransson, "The impact of wind power variability on the least-cost dispatch of units in the electricity generation system," Doctoral Thesis, Department of Energy and Environment, Chalmers University of Technology, Gothenburg, Sweden, 2014, ISBN: 978-91-7597-001-1. [Online]. Available: https://publications.lib.chalmers.se/records/fulltext/196126/196126.pdf.

[45] Danish Energy Agency, *Technology data - analyses and statistics*, Accessed: 2025-05-21, 2024. [Online]. Available: https://ens.dk/en/analyses-and-statistics/technology-catalogues.

[46] G. D. Ulrich and P. T. Vasudevan, *Chemical Engineering Process Design and Economics: A Practical Guide*, 2nd ed. Durham, N.H.: Process Publishing, 2004, p. 706, ISBN: 0970876823.

[47] L. Göransson *et al.*, "Tre elsystem som kan möta omställningen av industri- och transportsektorerna," Chalmers tekniska högskola, Mistra Electrification, Göteborg, Sverige, Rapport, May 2025, Institutionen för Rymd-, geo- och miljövetenskap, avdelning Energiteknik och Institutionen för Elkraftteknik.

[48] Statisktiska Centralbyrån, *Kommunal och regional energistatistik*, Accessed: 2025-05-23. [Online]. Available: https://www.scb.se/hitta-statistik/statistik-efter-amne/energi/energibalanser/kommunal-och-regional-energistatistik/.

[49] Energimarknadsinspektionen, *Energiskatt*, 2025. [Online]. Available: https://ei.se/konsument/el/elmarknaden/energiskatt.

[50] Konsumenternas Energimarknadsbyrå, *Energiskatt - skattesatser och kostnader*, Accessed: 2024-05-22, 2025. [Online]. Available: https://www.energimarknadsbyran.se/el/dina-avtal-och-kostnader/elrakningen/energiskatt-skattesatser-och-kostnader/.

[51] J. Öljemark, *Elskatt*, Accessed: 2024-05-22, 2025. [Online]. Available: https://www.ekonomifakta.se/sakomraden/elfakta/styrmedel/elskatt_1208668.html.

[52] V. SKATT, *Punktskatt på elström – företagskunder*, Accessed: 2024-05-22, 2025. [Online]. Available: https://www.vero.fi/sv/foretag-och-samfund/skatter-och-avgifter/punktbeskattning/elstrom-och-vissa-branslen/.

[53] G. Energi, *Därför byggde vi göteborgs största termos*, 2025. [Online]. Available: https://www.goteborgenergi.se/i-var-stad/artikelbank/darfor-byggde-vi-goteborgs-storsta-termos.

A

Appendix

A.1 Additional constraints used in the model

Table A.1: Description of constraints used in the model

Constraints	**Description of constraints**
Import/export capacity	Limits electricity import and export to the grid import capacity of each electricity region. $$-M_e^{El,\ cap} \leq w_{e,t}^{imp} \leq M_e^{El,\ cap}$$ $$\forall e \in E, \forall t \in T$$
Maximum production, electricity	The generation of electricity by a technology is lower than the installed capacity of said technology. $$p_{i,e,t} \leq s_{i,e}$$ $$\forall\ i \in I_{el}, \forall\ e \in E, \forall\ t \in T$$
Maximum production, heat	The generation of heat by a technology is lower than the installed capacity of said technology. $$q_{i,h,t} \leq s_{i,h}$$ $$\forall\ i \in I_{heat}, \forall\ e \in E, \forall\ t \in T$$
Storage level, batteries	The storage level of batteries at a certain timestep is the storage level at the previous timestep, plus or minus charging and discharging. $$SOC_{e,t}^{bat} = SOC_{e,t-1}^{bat} + b_{e,t}^{ch} - b_{e,t}^{dch}$$ $$\forall\ e \in E, \forall\ t \in T$$
Maximum storage, batteries	The storage level in a battery cannot exceed the capacity of the battery. $$SOC_{e,t}^{bat} \leq s_{bat,e}$$ $$\forall\ e \in E, \forall\ t \in T$$
Charging/discharging, batteries	The electricity charged or discharged from a battery cannot exceed its discharge capacity. $$b_{e,t}^{ch},\ b_{e,t}^{dch} \leq s_{bat,\ cap}$$

Constraint	**Description of constraint**
	$\forall\ e \in E, \forall\ t \in T$
Storage level, TES	The storage level of a TES at a certain timestep is the storage level at the previous timestep, plus or minus charging and discharging. $$SOC^{TES}_{h,t} = SOC^{TES}_{h,t-1} + TES^{ch}_{h,t} - TES^{dch}_{h,t}$$ $$\forall\ h \in H, \forall\ t \in T$$
Maximum storage, TES	The storage level in a TES cannot exceed the capacity of the TES. $$SOC^{TES}_{h,t} \leq s_{TES,h}$$ $$\forall\ h \in H, \forall\ t \in T$$
Charging/discharging, TES	The heat charged or discharged from a TES cannot exceed its discharge capacity. $$TES^{ch}_{h,t},\ TES^{dch}_{h,t} \leq s_{TES,\ cap}$$ $$\forall\ e \in E, \forall\ t \in T$$

A.2 Reference Case

A.2.1 No WHR

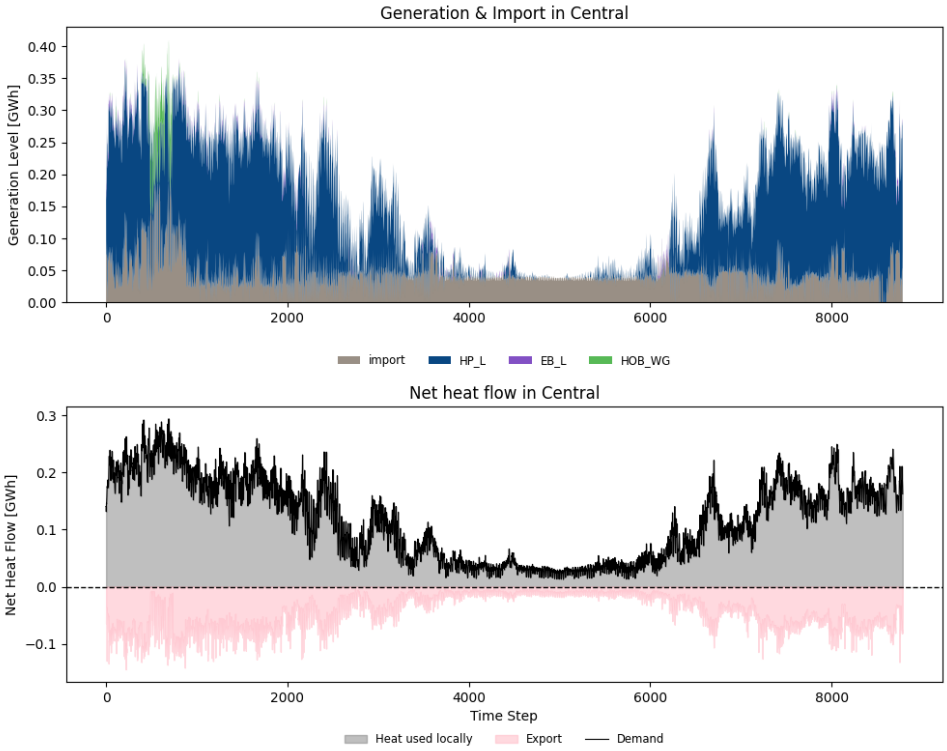

Figure A.1: Annual generation- and export of heat in region Central (no WHR).

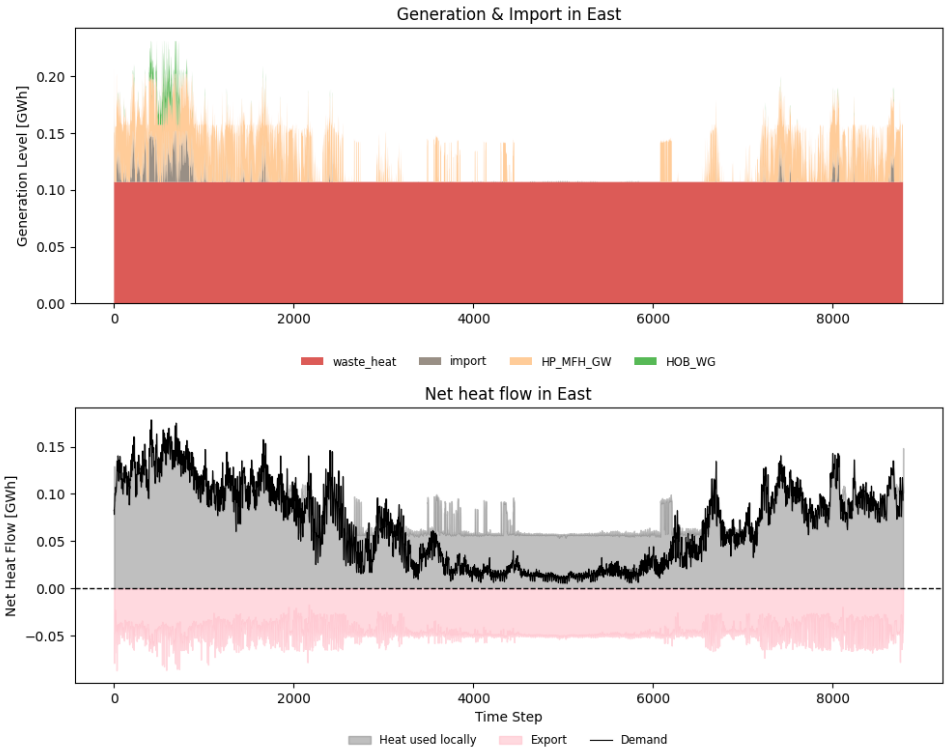

Figure A.2: Annual generation- and export of heat in region East (no WHR).

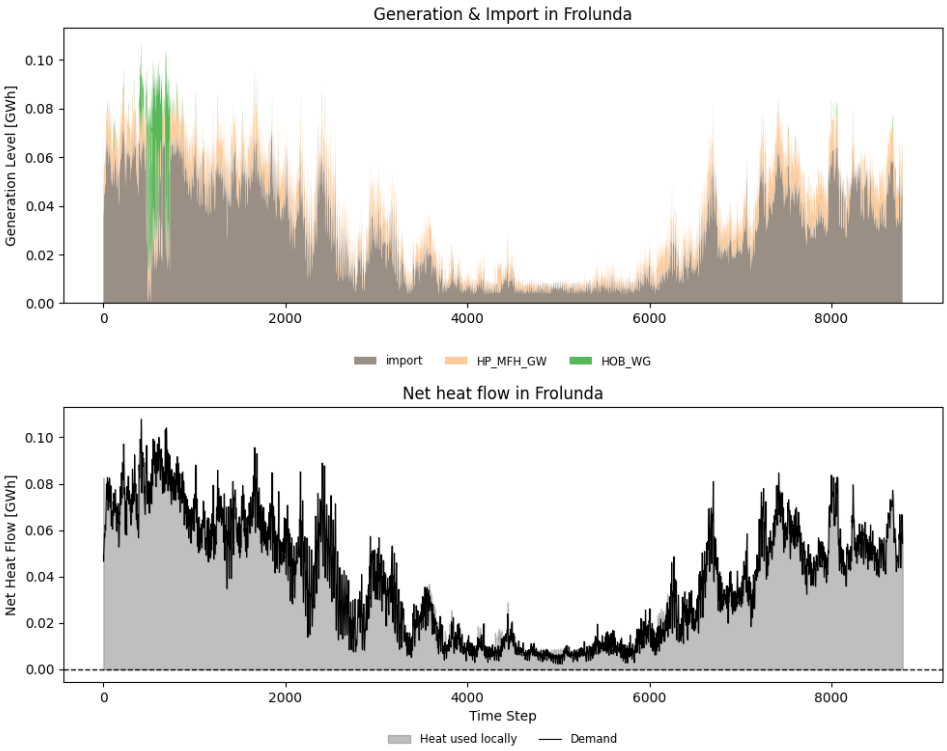

Figure A.3: Annual generation- and export of heat in region Frölunda (no WHR).

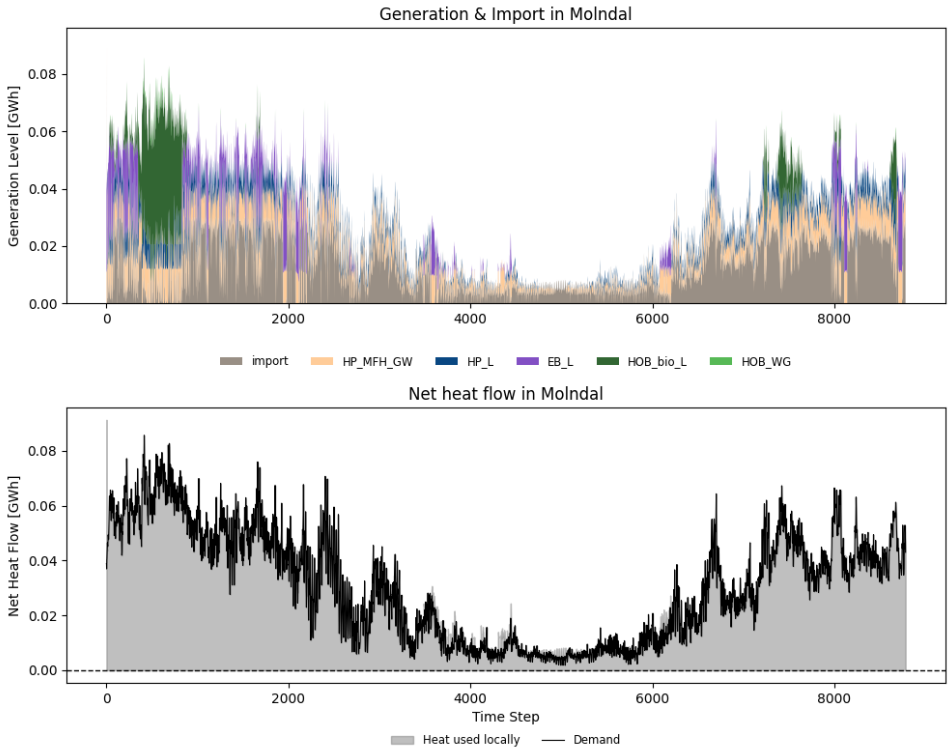

Figure A.4: Annual generation- and export of heat in region Mölndal (no WHR).

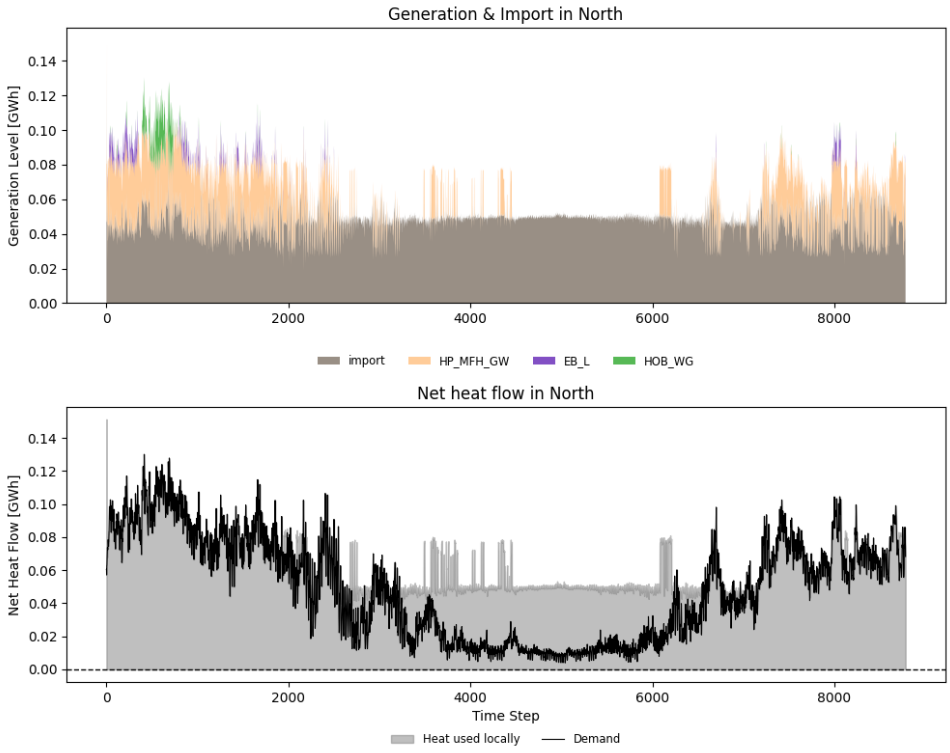

Figure A.5: Annual generation- and export of heat in region Northl (no WHR).

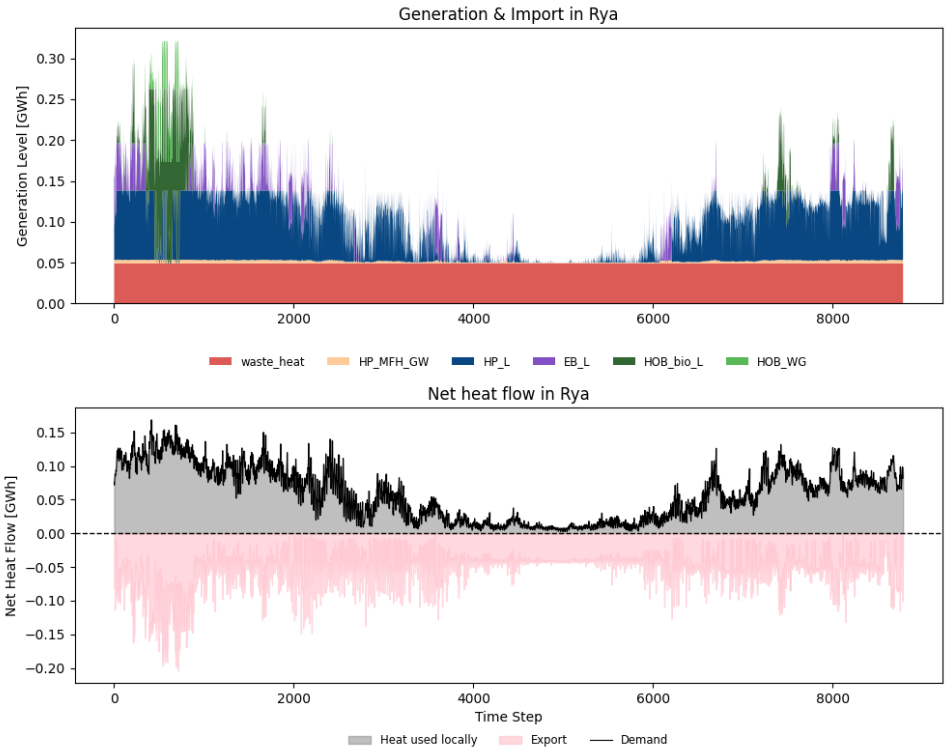

Figure A.6: Annual generation- and export of heat in region Rya (no WHR).

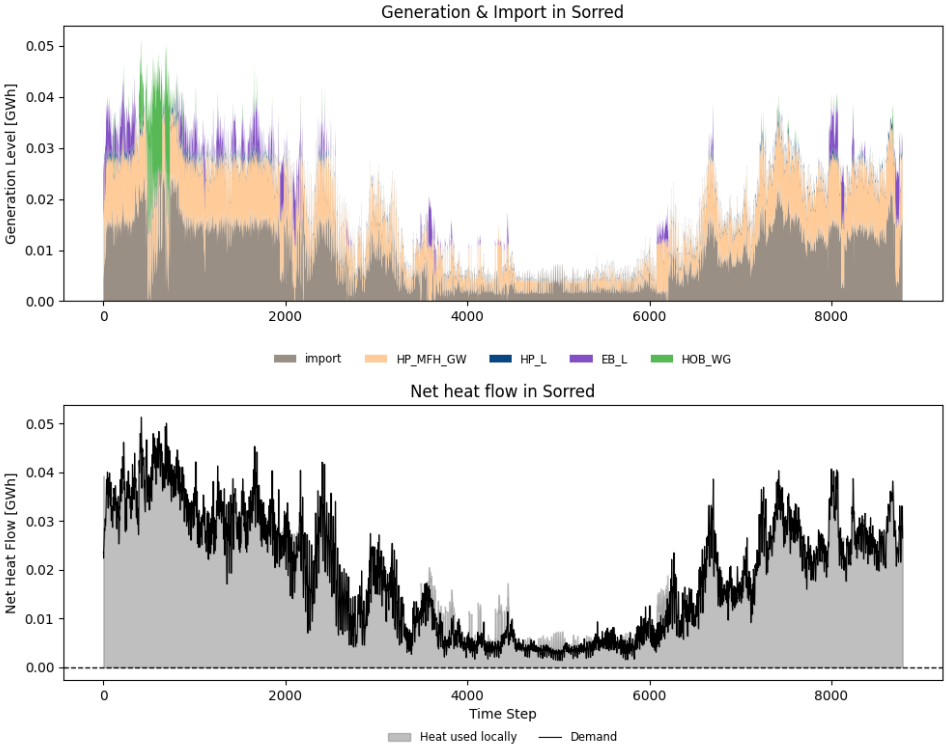

Figure A.7: Annual generation- and export of heat in region Sörred (no WHR).

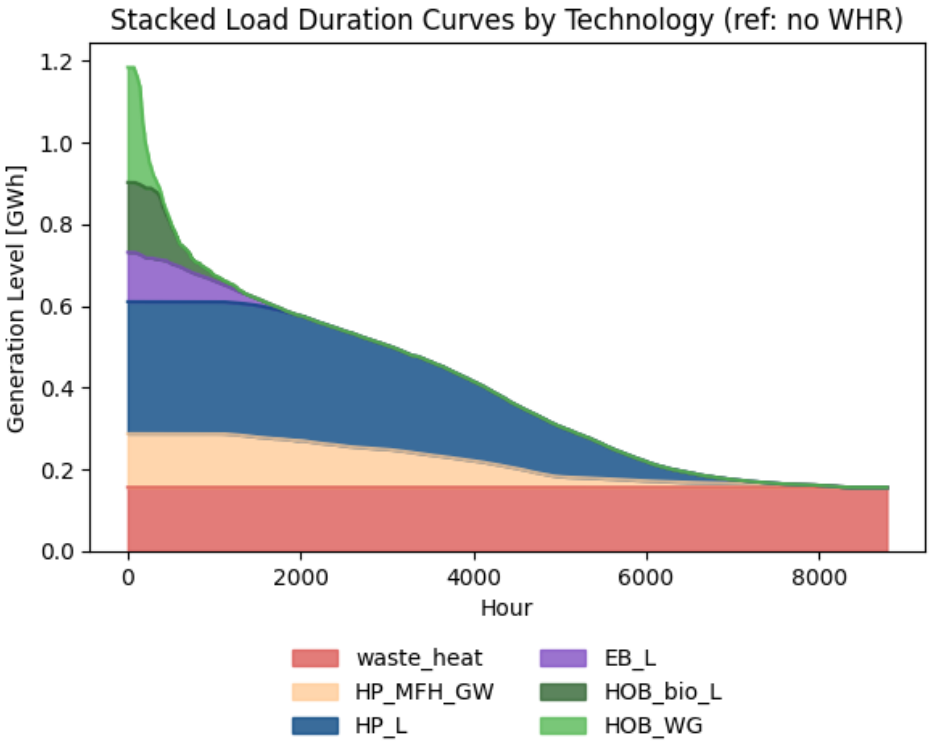

Figure A.8: Load duration curve of heat generating technologies in Gothenburg (no WHR).

A.2.2 WHR

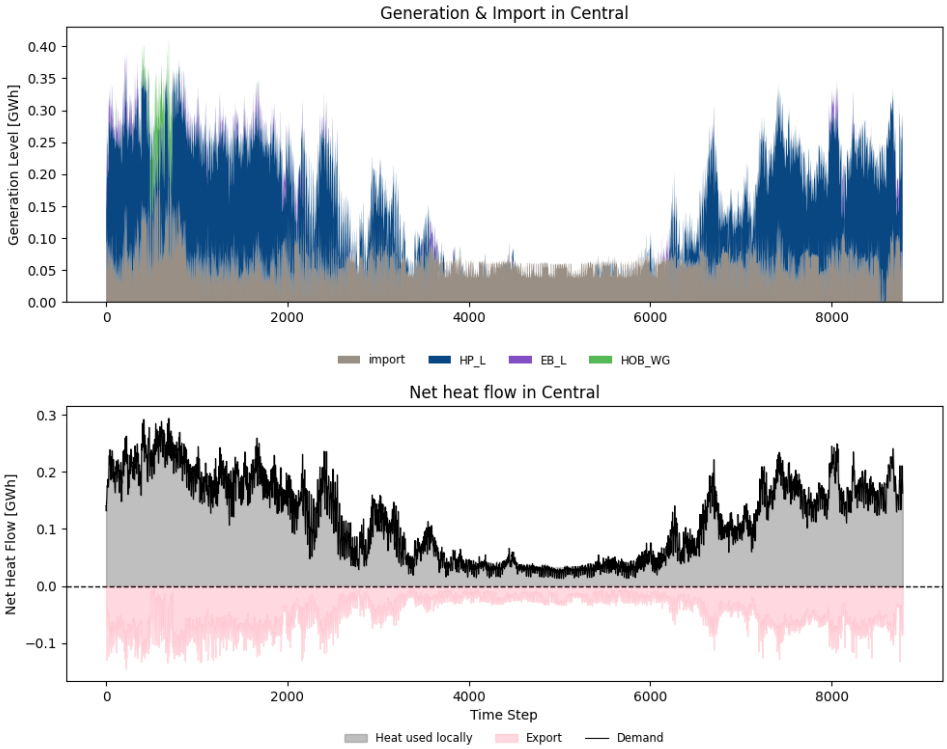

Figure A.9: Annual generation- and export of heat in region Central (WHR).

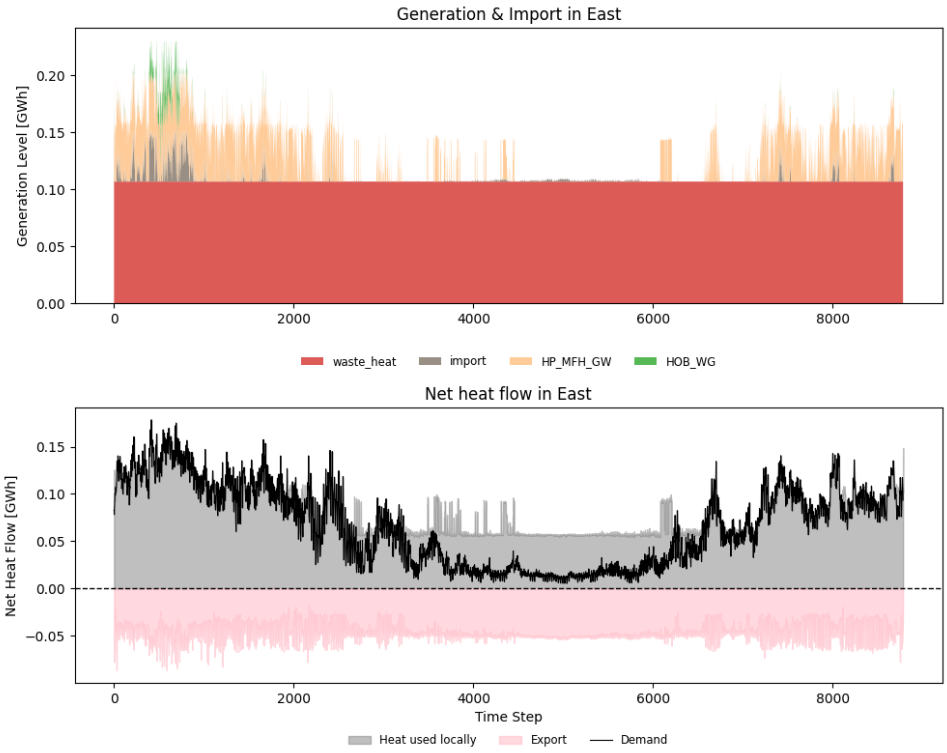

Figure A.10: Annual generation- and export of heat in region East (WHR).

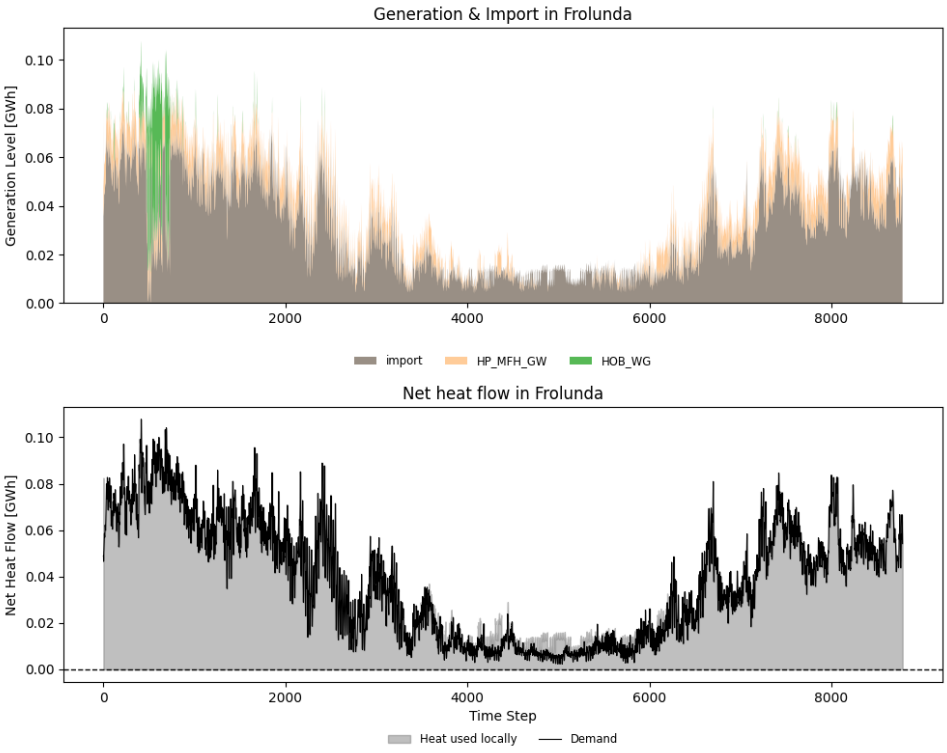

Figure A.11: Annual generation- and export of heat in region Frölunda (WHR).

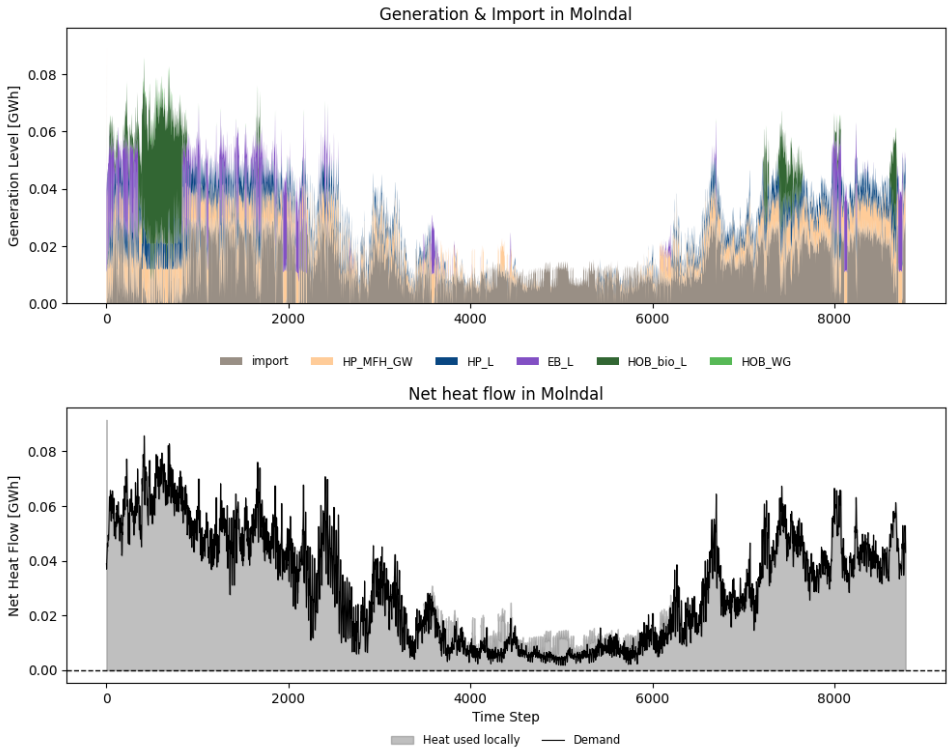

Figure A.12: Annual generation- and export of heat in region Mölndal (WHR).

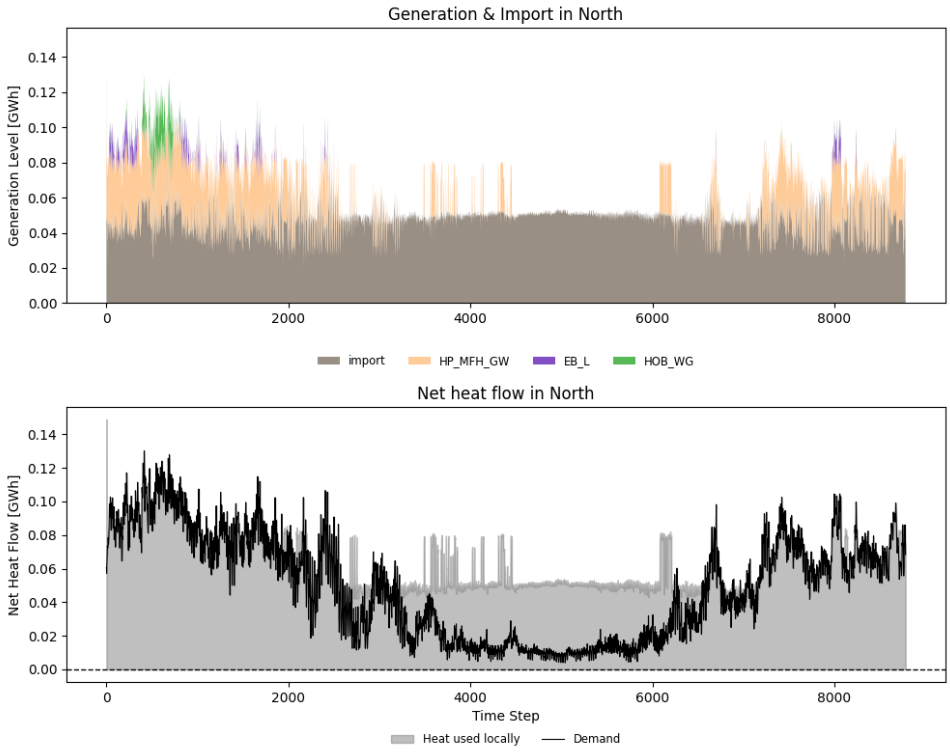

Figure A.13: Annual generation- and export of heat in region North (WHR).

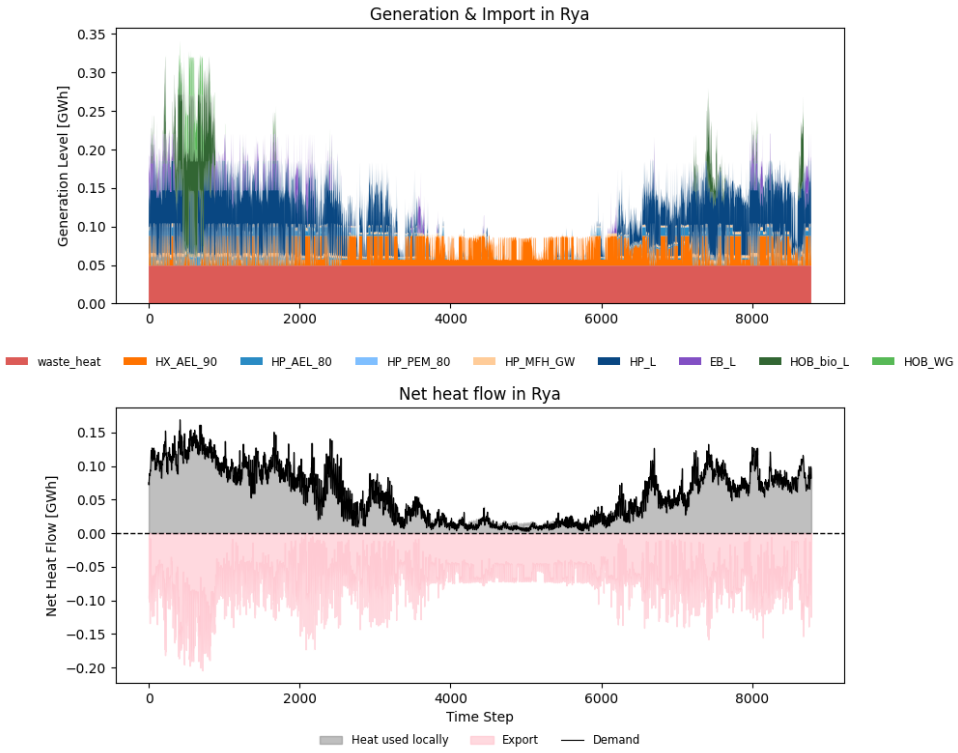

Figure A.14: Annual generation- and export of heat in region Rya (WHR).

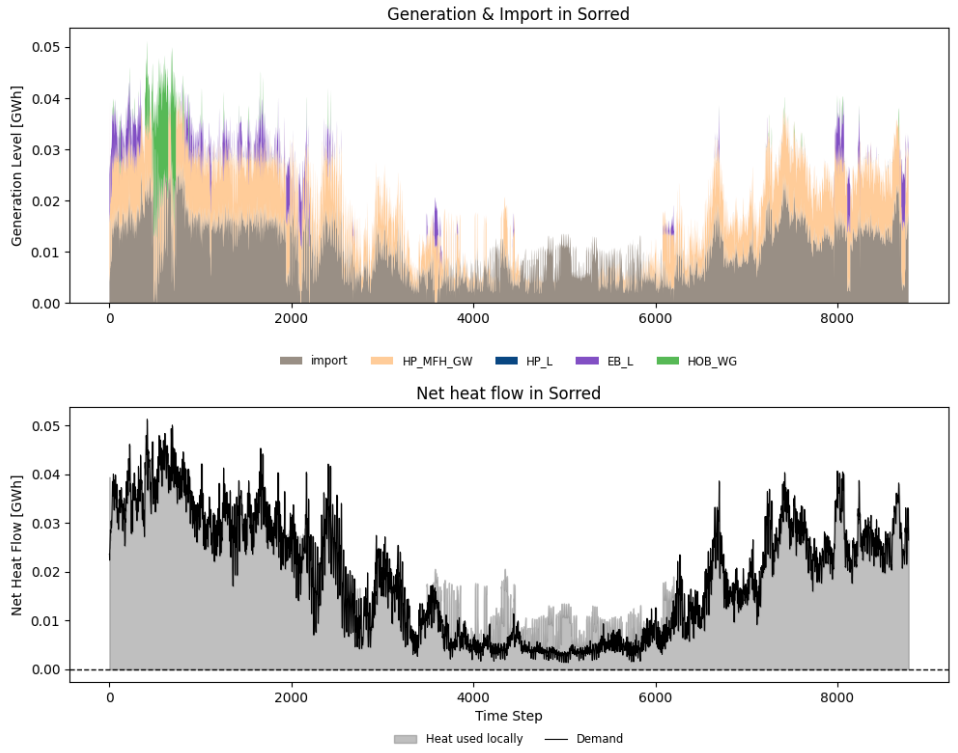

Figure A.15: Annual generation- and export of heat in region Sörred (WHR).

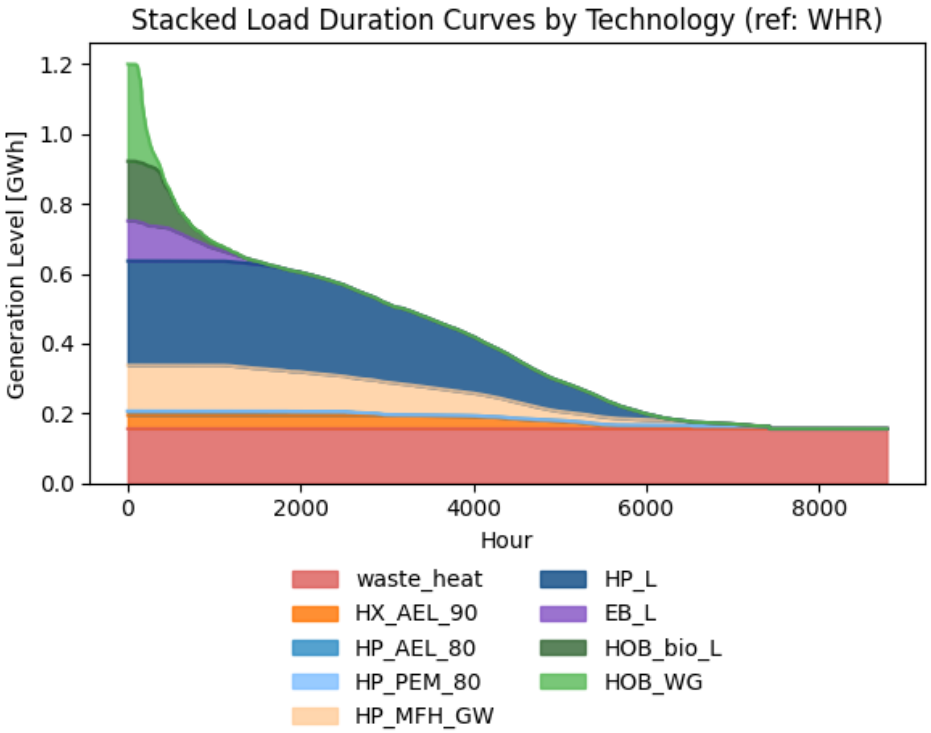

Figure A.16: Load duration curve of heat generating technologies in Gothenburg (WHR).

A.3 Sensitivity analysis

A.3.1 No hydrogen storage

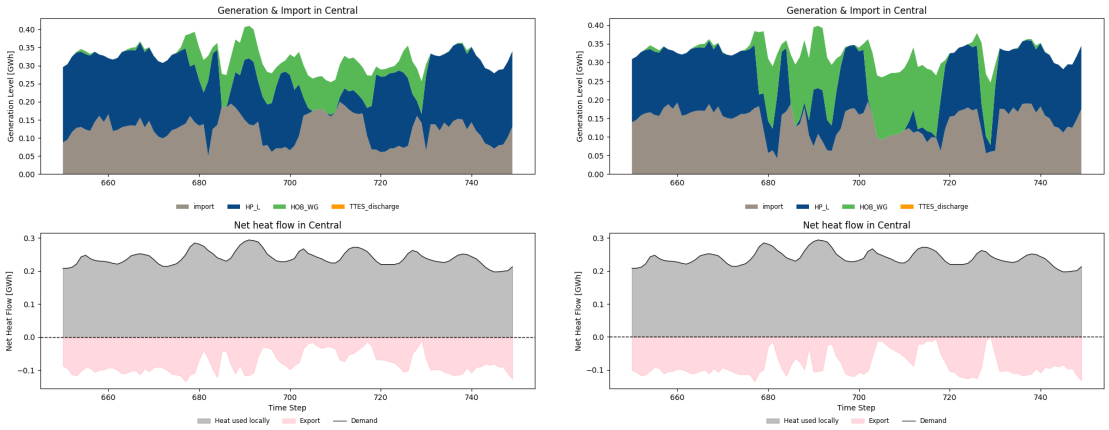

(a) **(b)**

Figure A.17: (a) and (b) shows the generation of heat in the central region during a high electricity price event (peak of 660 [EUR/MWh]) with- and withouth access to hydrogen storage respectively.

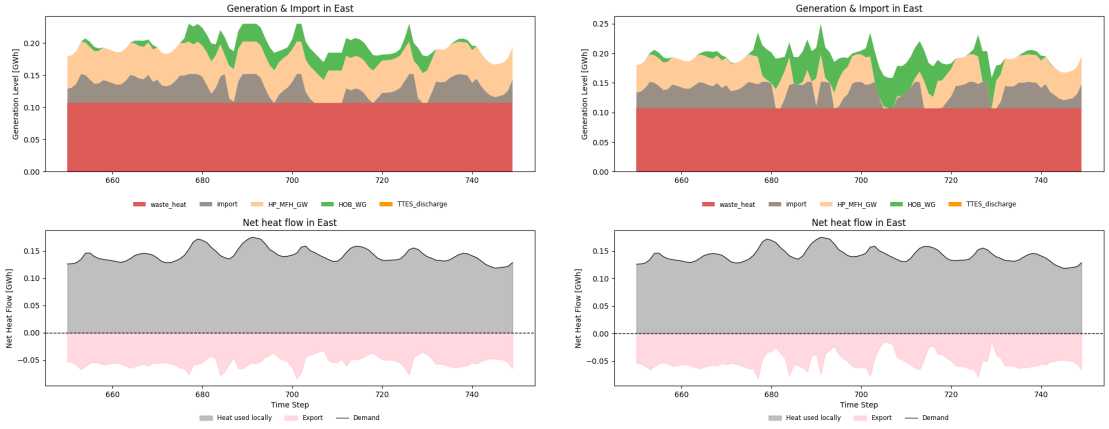

(a) **(b)**

Figure A.18: (a) and (b) shows the generation of heat in the east region during a high electricity price event (peak of 660 [EUR/MWh]) with- and withouth access to hydrogen storage respectively.

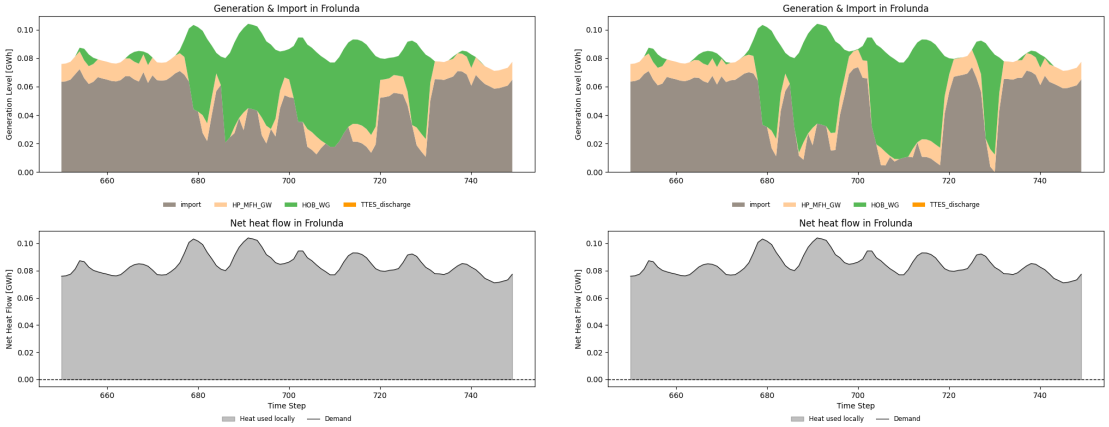

(a) **(b)**

Figure A.19: (a) and (b) shows the generation of heat in the Frölunda region during a high electricity price event (peak of 660 [EUR/MWh]) with- and withouth access to hydrogen storage respectively.

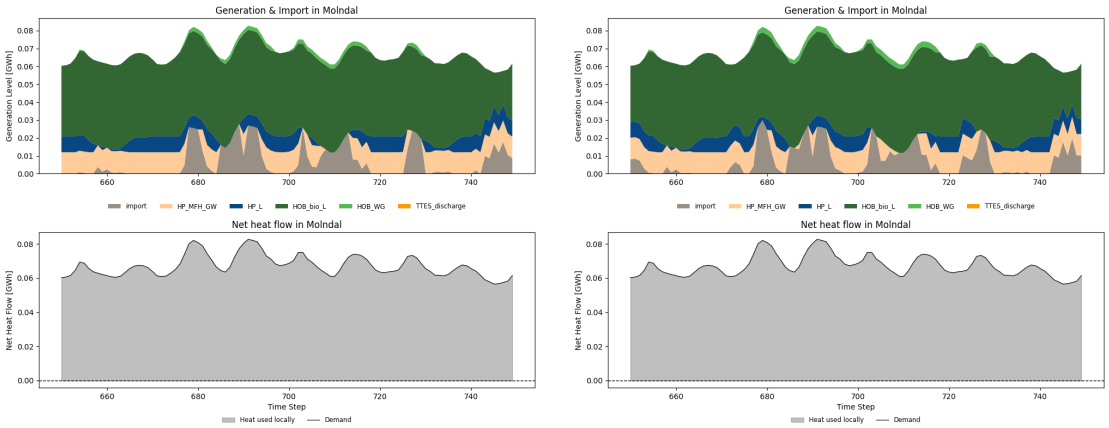

(a) **(b)**

Figure A.20: (a) and (b) shows the generation of heat in the Mölndal region during a high electricity price event (peak of 660 [EUR/MWh]) with- and withouth access to hydrogen storage respectively.

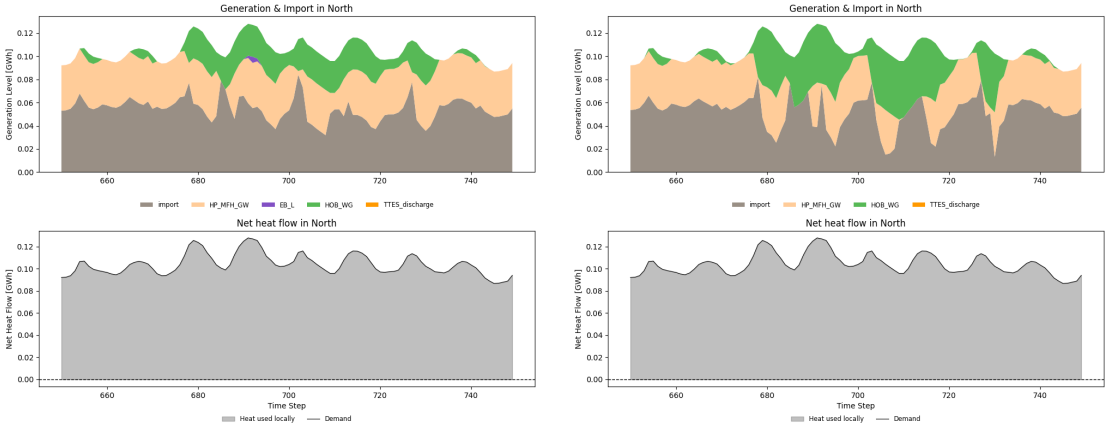

(a) **(b)**

Figure A.21: (a) and (b) shows the generation of heat in the north region during a high electricity price event (peak of 660 [EUR/MWh]) with- and withouth access to hydrogen storage respectively.

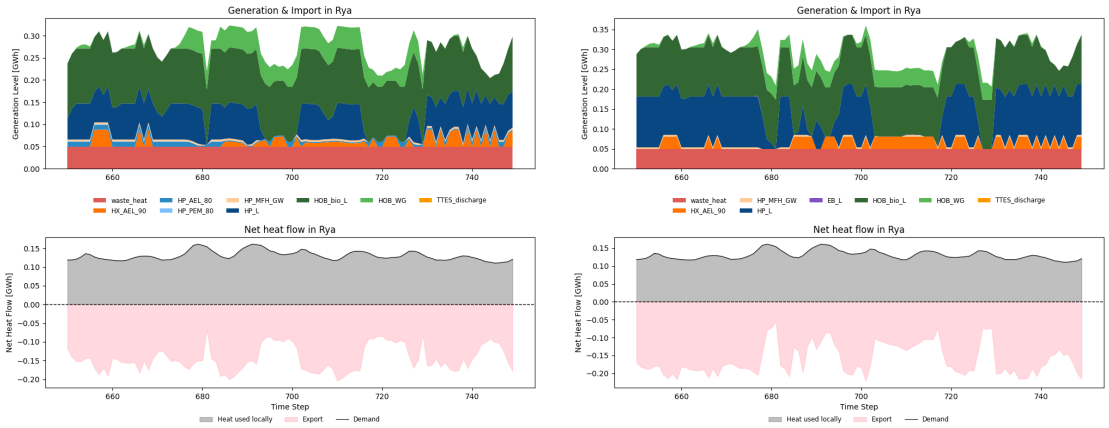

(a) **(b)**

Figure A.22: (a) and (b) shows the generation of heat in the Rya region during a high electricity price event (peak of 660 [EUR/MWh]) with- and withouth access to hydrogen storage respectively.

DEPARTMENT OF SPACE, EARTH AND ENVIRONMENT
CHALMERS UNIVERSITY OF TECHNOLOGY
Gothenburg, Sweden
www.chalmers.se

CHALMERS
UNIVERSITY OF TECHNOLOGY